Engineering Structures 237 (2021) 112231

Contents lists available at ScienceDirect

Engineering Structures

journal homepage: www.elsevier.com/locate/engstruct

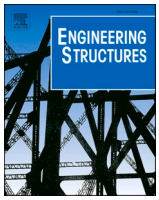

Review article

Sensors for process and structural health monitoring of aerospace composites: A review

Helena Rocha [a,*], Christopher Semprimoschnig [b], João P. Nunes [a]

[a] Institute for Polymers and Composites, University of Minho, Campus de Azurém, 4804 – 533 Guimarães, Portugal
[b] European Space Agency, Keplerlaan 1, NL – 2200 AG Noordwijk, the Netherlands

ARTICLE INFO

Keywords:
Structural health monitoring
Process monitoring
Optical fibre sensors
Piezoelectric sensor
Piezo–resistive sensor
Polymer composite
Sensor embedment
Aerospace application

ABSTRACT

Structural Health Monitoring (SHM) is a promising approach to overcome the unpredictable failure behaviour of composite materials and further foster their use in aerospace industry with increased confidence. SHM may require a complex system, including sensors, wiring and cabling, data acquisition devices and software, data storage equipment, power equipment and algorithms for signal processing, involving a multidisciplinary team for its adequate development considering the operational environment and requirements of a certain application. This review paper focuses on the most promising type of sensors, laboratory made and commercially available, for SHM of aerospace composites. Sensing principles, characteristics, embedding procedures, sensor/ host materials interactions and acquired sensor data/ material behaviour are discussed. The use of sensors for in-situ process monitoring, specifically for curing and mould filling monitoring in liquid composite moulding processes are discussed. General considerations for the development of SHM systems for the aerospace environment are also briefly mentioned.

1. Introduction

The use of FRP (fibre reinforced polymer) composites has been increasing in the last few decades to replace metal structures in aerospace applications, where commercial aircrafts, the Airbus A350-XWB and Boing 787, have reached more than 50% in weight of composite materials. The replacement of metals by FRPs intends to decrease weight of structural parts, to ultimately reduce fuel consumption and CO_2 emissions, and consequently, decrease costs. Aerospace composites present great strength and modulus provided by the reinforcing fibres. Generally, carbon fibres (CF) are used, but glass, aramid and boron fibres may also be used. Furthermore, the matrix provides corrosion and weathering resistance. Thermoset epoxy resin is often used but other examples for aerospace composites are polyester, phenolic and polyimide resins [1]. Thermoplastic polymers, specially the polyketone polymer family, such as polyetheretherketone (PEEK) and Polyaryletherketone (PAEK), are being considered as they may introduce manufacturing benefits, eliminating the need for autoclave and shortening the manufacturing cycles from hours to minutes [2].

Although composite materials hold promising achievements, their failure mechanisms are yet difficult to predict, as they may fail differently depending on whether they are under tension or compression, as opposed to metals, which tend to fail due to fatigue cracking [1]. Despite composite materials being less prone to fatigue damage than metals, it might still occur as they may face harsh environmental conditions during their lifetime. The fatigue behaviour does not only depend on matrix and fibre materials, but also on the layup sequence, which may vary from part to part, making it very difficult to get reliable data that could be generically applied to any part [1,3]. Another drawback of aerospace composites is their propensity to barely visible impact damage (BVID), that may result from impacts from bird strikes, hail, gravel and maintenance tools. These occurrences may ultimately lead to front face damage, and of more concern, matrix cracks, delaminations and/or fibre breakage that can go undetected by the human eye [4]. The eventuality of unpredicted failure on a composite aircraft structure often requires an over engineered design to comply with the rigorous and exigent safety rules of aerospace industry, particularly for civil aircraft, counteracting the initial purpose of using composites for weight reduction [5].

Structural health monitoring (SHM) of aerospace composites, through surface mounted or embedded sensors, is of great importance to prevent the issues mentioned above [1]. Embedding sensing systems in

* Corresponding author.
E-mail address: helenarocha@dep.uminho.pt (H. Rocha).

https://doi.org/10.1016/j.engstruct.2021.112231
Received 4 July 2020; Received in revised form 31 January 2021; Accepted 8 March 2021
Available online 4 April 2021

the composite structure, capable of detecting critical parameters, such as strain or temperature changes, improves the ability to monitor in–service structural health and, possibly, the manufacturing process as well, in contrast to surface mounted sensors. This provides a clear alternative to existing non-destructive evaluation (NDE) methods, which are typically used at the end of major process steps and their application is limited by the size of the structure. The embedment of sensors provides extra protection against surrounding operational environment, resulting in increased lifetime of the sensors [6]. SHM sensor technology is a cost-effective approach and increases the lifetime of the composite structure, as it can provide continuous data to repair and maintain the part in a timely manner, reducing unnecessary maintenance operations of aircraft structures [1].

Moreover, adhesive bonding is currently still not a fully accepted solution for mechanical fasteners replacement. The extensive safety requirements for civil aircrafts requires to test every single adhesively bonded joint produced to prove that it wouldn't detach and lead to structural failure in case the critical design load is applied, turning it a very expensive procedure [7]. While adhesive bonding may offer improved fatigue resistance, lighter weight, possibility to bond different parts and improved damping properties, at a reduced manufacturing cost, it may suffer degradation over time under harsh environments or by incorrect bonding, which might form a weak point during load transferring, that may eventually lead to detachment [8]. Recent research [9–11] investigating the application of SHM systems on adhesive bonds for debonding and defect detection may accelerate its use on aerospace primary structures.

Naturally, SHM technologies are still under development, and with great challenges to overcome. To accurately detect damage, the embedded sensor and the host composite structure must present good mechanical bonding, so that the sensor is subject to the same strain variation as the host structure, and the sensor must be close to the damaged area.

The present paper reviews the main types of sensors used in SHM of aerospace composite structures, namely fibre optic, piezoelectric and piezo-resistive sensors, and their characteristics, working principles, embedding procedures, and interactions with host materials. Both laboratory made and commercially available sensors are reviewed. Sensing approaches for process monitoring, with focus on curing monitoring and mould filling monitoring for liquid composite moulding (LCM) processes, are also reviewed. Some considerations regarding the development of SHM systems for composites for aerospace applications are briefly highlighted.

2. Aerospace environment

The impact of high velocity space debris and micrometeroids on a spacecraft might jeopardize the structural integrity and performance of the system, as damage may arise from consecutive impact events [12]. As mentioned before, heavy hail on aircraft structures may as well lead to several damage modes, such as transverse cracks and delamination [4]. In-flight conditions may cause shape deformation of wings of unmanned aerial vehicles (UAV) or commercial aircrafts [13].

The implementation of SHM systems is essential to ensure that the interrogated structures can perform properly and survive the harsh aerospace environment they are exposed to throughout their working lifetime. Generally, aerospace applications require light weight, small and low-power consuming monitoring systems that are immune to electromagnetic interference [13]. The diverse nature of mechanical solicitation taking place at the different stages of a flight in aircraft structures, requires data acquisition systems with a wide scan rate range, from hundreds to thousands of hertz. Such requirement arises from the fact that operational strains, to detect nonconformities on the predicted fatigue life, involve measurements in the order of thousands of με and can be achieved at low scan rate, whereas the detection of impact damage or delamination needs a high scan rate system [13]. Whilst SHM techniques are novel and helpful, their in-service reliability is not fully developed yet. Moreover, typical air and spacecraft manufacturing processes do not currently consider embedding smart sensors in their design. The uptake of SHM becomes challenging when the product is already manufactured. Yet, surface mounted sensors could be a viable solution in some cases.

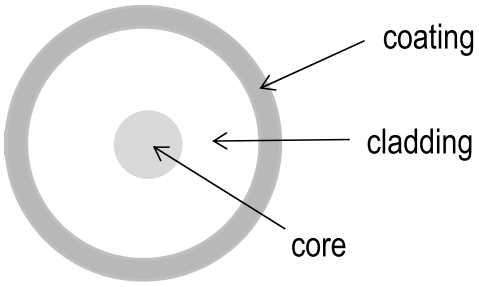

Fig. 1. Schematic of cross-sectional area of an optical fibre.

3. Sensors for structural health monitoring

A sensor for SHM should fulfil a few basic specifications: (1) it should only monitor the real damage condition of the host structure and be independent to changes in the environment; (2) it should transmit the acquired signals reliably; (3) it should produce as little impairment as possible on the host structure; (4) it should survive the surrounding work environment for at least as long as the service life of the host structure; and (5) it should be easy to handle, attach, integrate and operate. Furthermore, sensors for SHM of aerospace structures require additional features, such as small dimensions, light weight, long service life with ageing resistance, low power consumption, good signal-to-noise ratio, compact wiring or wireless construction, and preferably have low cost [14].

3.1. Fibre optic sensors

The occurrence of damage may result in a change of strength and stiffness, which can be revealed by fibre optic strain sensors by a change in their optical properties, such as intensity, wavelength, phase or state of polarization, following a linear relation with the mechanical axial strain [15–18]. Fibre optic sensors (FOS) can be either embedded or bonded to the structure. FOS present several advantages, they are immune to electromagnetic interference, small, light, durable, and have high bandwidth, which allows multiplexing sensors in the same optical fibre (OF) [13,19]. Despite FOS can be made of simple cheap telecom optical fibres, the optoelectronic interrogation systems used for measurement and processing of the optical signals are still very costly [13]. The sensitivity of OF to moisture and chemicals require them to be coated by a polymeric film for protection, making the outer-diameter of the fibres very large, greater than at least ten times that of the diameter of the reinforcing fibres in the composite material [20].

Optical fibres are composed of a silica core of higher refractive index to restrain the light within itself, surrounded by a silica cladding of lower refractive index, and externally protected by a coating of polymeric materials, as previously mentioned. A schematic representation of the cross-sectional area of an OF is presented in Fig. 1. Depending on the diameter of the internal core, the OF are classified as single-mode, with a core diameter of about 10 μm and capability to carry only one mode of the light wave, and multimode fibres, with core diameters varying from 50 to 100 μm, allowing to carry more than one mode of the light wave. While multimode OF sensing range can be greater, they have lower accuracy and require higher light intensity, as opposed to single-mode OF, which can reach a distance of about 40–50 mm away from the sensor, with higher sensitivity, required for strain measurements [21]. Chambers et al. [22] reported an fibre Bragg grating (FBG) sensor

Table 1
Characteristics summary of different fibre optic sensor types.

Type of sensor	Advantages	Disadvantages	Observations	Applications
Interferometric Fabry-Perot sensor	High strain resolution	Hardly multiplexed, cross temperature-strain sensitivity, fragile	Numerous cavity solutions possible for cross temperature sensitivity issue	Strain, temperature, vibration, cure monitoring
Grating-based sensors (e.g. FBG)	Discrete measurements of strain and temperature over large areas and at selected needed locations, well know technology	Cross temperature-strain sensitivity, limited damage severity and location assessment	Typical strain sensitivity of 1.2 pm/με and temperature sensitivity of 10 pm/°C	Temperature and strain measurements, low velocity impact damage detection, damage localization, cure monitoring
Distributed sensors	Measurements at any location along the fibre length, potential to monitor an entire aircraft, suitable for monitoring of large area composites	Expensive interrogation systems, spatial resolution in the cm to m range	Careful sensing technology selection for each specific application is needed	Strain, temperature, vibration, delamination

capable of detecting residual strain from a low velocity impact event with an energy of 0.33 J, 10 mm away from the damaged area.

Fibre optic sensors can be classified according to their spatially-resolved measurement type as: interferometric sensors having single-point detection; grating-based sensors having quasi-distributed capabilities, able to make discrete measurements at sensor locations; and distributed sensors that can make measurements at any location along the fibre length. Interferometric sensors work based on an intrinsic or extrinsic cavity located along the fibre [23], which reflects a different optical phase between two interference light waves when physical changes occur in the host structure [15]. Common interferometric sensors are Fabry-Perot sensors, characterized by its high strain resolution, as high as 0.15 με, with strain measurement ranging up to ±5000 με, at operating temperatures from −40 to +250 °C, and being very compact with no weight penalty to the structure. However, they cannot be easily multiplexed. Another well-known example are low coherent interferometric sensors (SOFO sensors), yet they are not suitable for SHM of aircraft structures as they work best for measurement of deformations at a low speed, 0.1–1 Hz [15], whereas aircraft structures require measuring systems capable of reading deformations ranging from hundreds to thousands of hertz, to monitor both operational deformations and impact damage [13]. Distributed sensors are designated as optical time-domain reflectometry (OTDR), Raman optical time-domain reflectometry (ROTDR), and Brillouin optical time-domain reflectometry (BOTDR) as they are based on Rayleigh, Raman and Brillouin scattering principles, respectively. External loads cause changes in the magnitude of the reflected signal in the core/cladding interface, which can be directly related to a mechanical strain [15]. ROTDR based sensors can measure temperature with a resolution of 0.2 °C with a distance range of about 8 km, while BOTDR can measure both temperature and strain with a spatial resolution from 1 to 4 m and distance range of 30 km, which can be extended up to 200 km. A few grating-based sensors have been reported in the literature, but FBG sensors present the most matured technology [15]. FBG sensors have proved to be able to monitor low impact damage, either under static or dynamic deformation [22]. FBG sensors have the advantage over other types of FOS of being intrinsic sensing elements, as the obtained signal is encoded directly in the wavelength form, easing wavelength division multiplexing [19]. With multi-point measurements provided by grating-based sensors and distributed sensors, a large area of the structure can be monitored with reduced wiring, keeping it a light weight structure, as opposed to traditional strain gauges or piezoelectric sensors [13,19]. Table 1 highlights and compares the main characteristics of the aforementioned sensor classifications.

Due to the widespread use and research on FBG sensors, this section is focused on this technology for SHM. An FBG sensor consists in a narrowband reflector [24], obtained through a grating with a refractive index different of that of the core material, by writing it into the fibre

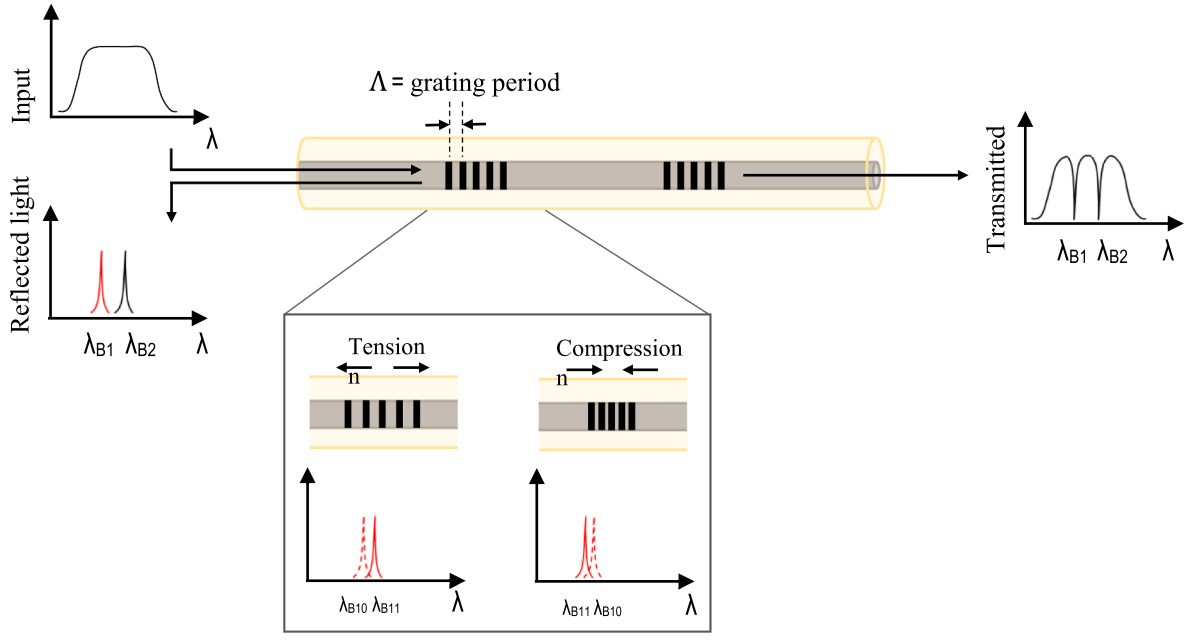

Fig. 2. Schematic representation of an OF with two FBG sensors, with illustrative graphs of the input light spectrum, transmitted spectrum with notch corresponding to the Bragg wavelength seen in the peak of the reflected spectrum. Illustration of the Bragg wavelength shift, as the grating period is increased or decreased, when OF is under tension or compression, respectively.

core surface, exposing the side of the fibre to ultraviolet light, working as wavelength specific mirror. These sensors are multiplexed by inscribing grating of such nature with periodically different refractive indexes and, consequently, different Bragg wavelengths. The FBG sensor length can be as small as 1 mm [25]. FBG can be directly inscribed into the fibre without affecting the fibre diameter, they are suitable for an extensive range of applications requiring small diameter probes, such as strain mapping of advanced composite materials. The operating principle of FBG sensors is depicted in Fig. 2.

FBG sensors are based on the Bragg's law, where the Bragg wavelength, λ_B, which is the reflected wavelength by a set of periodic gratings, is dependent on the effective refractive index of the grating, η_{eff}, and on the grating period, Λ, according to equation (1) [13].

$$\lambda_B = 2\eta_{eff}\Lambda \tag{1}$$

When a local deformation is induced, it leads to a variation on the grating period, resulting in a change on the reflected Bragg wavelength, allowing to detect the local strain, resorting to equation (2) [13].

$$\Delta\lambda_B/\lambda_B = (1-\rho_e)\varepsilon \tag{2}$$

being ε the longitudinal strain and ρ_e the photo-elastic coefficient of the fibre core material. For silica core fibres ρ_e is 0.22 and for a typical grating with a central wavelength of 1550 nm, the strain sensitivity is about 1.2 pm/μm [13].

The capability of FBG sensors to detect BVID has been demonstrated. A residual strain as low as 3 με has been detected by an FBG after an impact of 0.33 J, which did not produce any delamination or matrix cracking. Moreover, the residual strain increased to 25 and 605 με for impacts with energies of 1.67 and 2.99 J, respectively, which lead to matrix cracking and delaminations. Fibre breakage was also detected by microscopic analysis and ultrasonic C–Scan in the samples exposed to 2.99 J impact energy [22]. It should be added that the impact energy that produces detectable damage depends on the properties and structure of the composite laminate, and on the distance between the FBG and the impact location and, thus the same impact energy can induce very distinct damage severity on composites having different lay-up configuration. In some cases, damage location has also been assessed by the time of arrival (TOA) method. Hafizi et al. [16] reported the use of a two-channel system, an optical fibre with two NIR-FBG sensors, for impact location on a 4 mm thick glass fibre (GF)/ epoxy composite laminate. The TOA method, considering a one-dimensional structure with two sensors, equation (3), was used to calculate the linear impact location.

$$l_2 = 1/2 \times (\Delta t \times Cg + L) \tag{3}$$

where l_2 is the distance between sensor 2 and impact location, Δt is the time difference between the arrival of the signal peaks of each sensor, Cg is the group velocity of the waves travelled on the sample, determined from the dispersion curves of the sample, and L is the distance between the sensors. Additional investigations of the signals utilising continuous wavelet transform, allowed to conclude that this system was able to locate linear impact sources with a relative error under 10%. Entire structures can be instrumented with multiple FBG sensors. Güemes et al. [26] have instrumented a lattice structure, envisioned for space applications, having a height of 1100 mm and diameter of 800 mm, and produced by automatic tape-laying process, with 36 FBG sensors. Strain values were acquired while the structure was fatigue loaded under compression. Although an initial failure broke a few bars, at –330 kN, the structure preserved its load-carrying capacity. The results revealed that minor production defects that produced an irregular strain distribution that led to a nonlinear behaviour under fatigue loading.

Although SHM of composite materials can bring a great advantage towards damage monitoring and safety, an adequate installation of this technology is imperative. A few concerns associated to the FBG technology are discussed below.

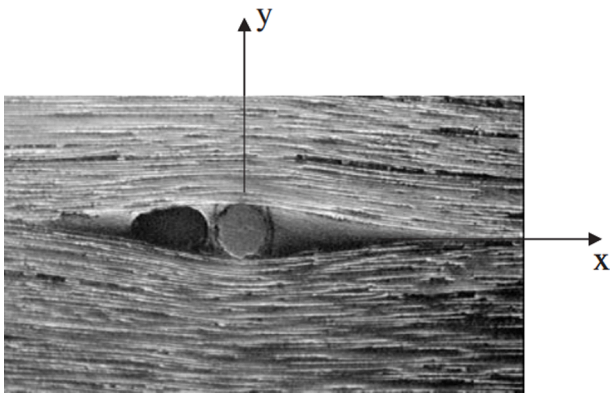

Fig. 3. Micrograph of the cross-section of an 8-ply unidirectional composite laminate embedded with FOS [27].

A detrimental embedding of FOS in the composite may lead to degradation of the mechanical properties and higher risk of failure of the composite material. Theoretically, the strength and modulus degradation of the composite material depend on the angle between the optical fibre and adjacent reinforcement plies, overall laminate thickness, diameter of the optical fibre and material of protective coating of the optical fibre [3]. The degradation of the mechanical properties is noteworthy for higher angles between the optical fibre and adjacent plies. The presence of "eye" patterns or voids in the resin, which are defects that may serve as trigger points of premature failure by delamination, may be produced when the optical fibre is embedded perpendicularly to the reinforcement fibres, as it can be seen in Fig. 3. Yet it will only be relevant for structures with high density of fibre optical sensors. On the contrary, there will be a uniform consolidation around the optical fibre if they are placed parallel to the reinforcement fibres, resulting on minimal defects and lower impairment of the composite mechanical properties, as the OF itself can also carry load [3].

The fact that the outer-diameter of an OF is about 10 to 15 times larger than the traditional carbon or glass fibre reinforcements raises some concern [3]. This issue has been surpassed by utilizing small-diameter optical fibres and a few studies have been reported in the literature with laboratory developed small-diameter optical fibres (SDOF) [28,29]. Commercial SDOF solutions, such as the T60 Small Diameter Fiber FBG from Technica [30], are still very scarce. Fig. 4 compares typical large diameter optical fibre (LDOF) with a SDOF, which are laid parallel to the reinforcing fibres of the carbon fibre reinforced polymer (CFRP) composite. It is possible to observe that the LDOF leads to poor consolidation of the reinforcing CF and formation of matrix rich regions [29].

The success of the embedding process of FBG sensors in composite structures is limited, as the signal may be weakened and the OF may break easily. Ramly et al [31]. embedded FBG sensors into sandwich composite structures, where the shifts of wavelength before and after embedment were generally lower than 1 nm, yet the signal showed a power drop within the OF after embedment. Optical connectors well suited for both the manufacturing process in industrial facilities and operational test conditions are required to ease the integration of optical fibres, specially at the ingress-egress point. Giraldo et al. [32] have reported the development of a trimmable optical connector which was integrated in a specimen simulating a root joint of a lower wing. The optical connector includes a connecting component that is embedded in the composite material, where the OF is hold and centred, and a protective element to seal and prevent the entry of resin into the connecting component. When the structure is cured and before trimming, the protective element can be removed and a second connecting component can be installed for the optical fibre to be interrogated. Another simple solution could be surface mounting the FOS. Although they would be directly exposed to the operational environment, encapsulating

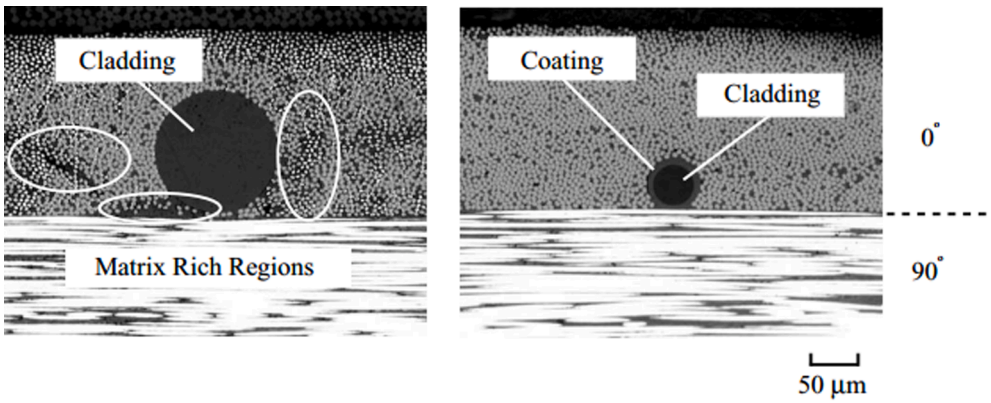

Fig. 4. Cross-sectional images of CFRP laminates embedded with (a) standard LDOF and (b) SDOF with FBG sensors [29].

protective materials could be used. Goossens et al. [33] have proposed the embedment of Ormocer® coated FBG sensors in a 1.0 mm diameter GFRP cylindrical profile, along the full length of the OF, for mechanical strength, with a 0.2 mm thick high-density polyethylene (HDPE) outer sheath, to inhibit humidity and oil ingress. The encapsulated FOS were pre-strained and adhesively bonded to thermoplastic CFRP specimens using a bi-component epoxy adhesive specially designed for optical fibres, and subsequently exposed to an annealing procedure to eliminate residual strains between the FOS and the protective GFRP coating. The instrumented specimens were then subjected to thermal cycling, pressure cycling, humidity exposure, hydraulic fluid exposure and fatigue testing, to mimic in-flight operational conditions. After testing, the specimens showed a positive shift of Bragg wavelength, which shows that a pre-strain is still applied on the encapsulated FOS and that the epoxy adhesive bond has not been damaged, although this could also be the result of increased temperature when the measurements were taken.

The Bragg wavelength shift is also affected by temperature, and it is still difficult to compensate for it without impairment of the fibre resolution [34]. A few approaches have been developed to compensate for the sensor sensitivity regarding temperature. The easiest approach comprises an additional strain free reference FBG sensor, where the temperature is measured, only useful if all FBG sensors are exposed to the same temperature. The method may be applied to both surface mounted and embedded sensors. If a strain free area is not accessible, a reference FBG sensor can be encapsulated in a capillary [13]. Glass capillaries have been demonstrated to be better suitable for temperature sensitivity isolation than stainless steel capillaries. The FBG sensor in a glass capillary has barely shown any sensitivity to heating rate changes and had the lowest thermal lag, when compared to FBG sensors in stainless steel capillaries [35]. FBG sensors of different grating structures, such as tilted FBG sensors [36], chirped FBG sensors [37,38], and birefringent FBG sensors [39], having various and independent peaks, have also been investigated to decouple strain and temperature influence on the wavelength shift. The latter approach may be valuable for applications requiring precise strain and temperature measurements at different points of the structure, with minimal OF length, whereas the use of strain free reference FBG sensor or encapsulated FBG sensor may not measure accurate temperature values if the temperature is not uniform in the whole structure. The temperature sensitivity of FBG sensors is about 10 pm/°C.

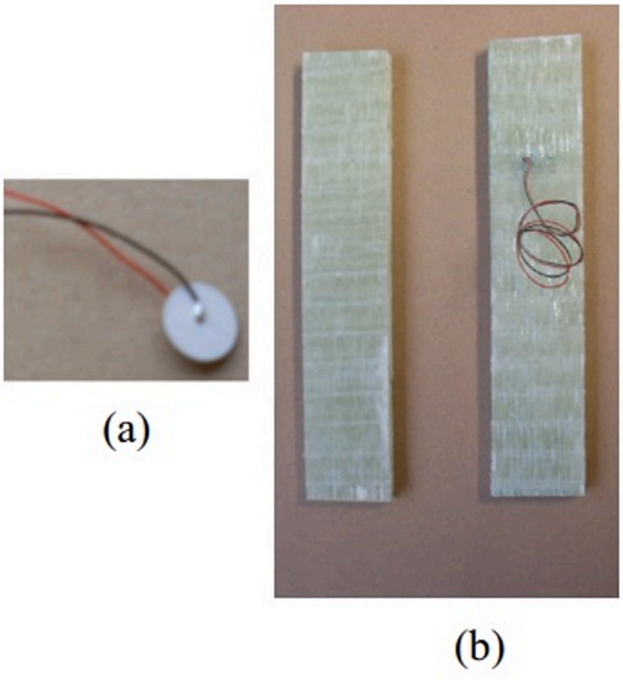

Fig. 5. SHM of GF/epoxy composite by PZT sensor: (a) PZT sensor; (b) blank GF/epoxy composite (left) and with embedded PZT (right). Adapted from [42].

The high sensitivity of FBG sensors to minor strains and temperature variations has fostered their wide use and acceptance for damage detection and cure monitoring, as also discussed in Section 4.1. However, in the authors' perspective, the embedding procedure and sensor placement should be carefully considered with special attention paid to the ingress and egress points of the OF in the host structure. This can be particularly problematic when using vacuum bagging techniques, such as the vacuum assisted resin infusion process. Solving the strain-temperature cross sensitivity issue is essential for accurate strain measurements. Although the use of a capillary encapsulated FBG sensor is the most straight forward and cost-effective approach, care must be taken when closing both ends of the capillary, to impede resin flowing in to the loose OF extremity inside the capillary. The very localized sensing nature of FBG sensors is advantageous for evaluation of localized damage but hinders the assessment of the overall structural condition.

3.2. *Piezoelectric sensors*

A piezoelectric material produces an electric charge when it is stressed, known as the direct piezoelectric effect, conferring sensing capability to these materials, by measuring changes in force, displacement, or velocity. Reciprocally, a piezoelectric material also presents a deformation when subject to an electric field, known as the converse piezoelectric effect, allowing the piezoelectric material to serve as an actuator and acoustic source generator [40]. This is a characteristic of dielectric materials with asymmetric crystalline structures, which occurs in some ceramics, polymers, and crystals, such as quartz, lithium sulphate, tourmaline and Rochelle salt. Ferroelectric ceramics, such as lead

zirconate titanate (PZT), and some polymers, such as polyvinylidene fluoride (PVDF), polyamides, polyimide and polyvinylidene chloride (PVDC), can be poled to obtain piezoelectric properties, by reorientation of the crystal structure or crystallites, respectively. The poling process consists in applying a high electric field at an elevated temperature, and then the material is allowed to cool down with the electric field still applied in order to keep the orientation state. The piezoelectric properties are lost when the material is subject to a high mechanical stress or electric field capable of reorient the structure and make it symmetric, or when it is heated above its Curie temperature [40,41].

Piezoelectric sensors offer high mechanical strength and operation for a wide frequency range, able to fulfil demanding applications, at low price and with small sizes. Piezoelectric sensors can be either surface mounted or embedded for superior longevity and higher sensitivity to damage, without prejudice of the mechanical properties of the host structure. Masmoudi et al. [42] compared the performance of surface mounted and embedded piezoelectric sensors on unidirectional and cross-ply E-glass fibres/epoxy composites produced by hand lay-up and examined the effect of the sensors on the mechanical properties of the host structure due to fatigue loading by acoustic emission. Acoustic emission is a highly sensitive technique for real time damage monitoring that analyses the transient ultrasonic waves generated as damage develops in the loaded structure, which are detected by the PZT sensors. The characteristics of the acoustic emission signals (energy, amplitude, rise time, counts and duration) are analysed to identify damage mechanisms. Fig. 5 (a) shows the piezoelectric sensor with a diameter of 5 mm and thickness of 0.5 mm and Fig. 5 (b) shows the neat E-glass fibre/epoxy composite and composite with embedded sensor in the neutral plane during manufacturing. Three stages of acoustic activity were distinguished in the composites for specimens with and without embedded sensor during fatigue tests. The first stage is characterized by an intense acoustic activity, attributed to the initiation of micro-cracks and its proliferation, with signal amplitudes between 43 and 95 dB. In the second stage there is a reduction in the acoustic activity, where the spread of micro-cracks, and likely fibre–matrix debonding, occur and corresponding to about 85% of the composite lifetime. The signals had amplitudes between 60 and 98 dB. The last stage is characterized by a brief and intense acoustic activity, having high energy signals with amplitudes exceeding 88 dB. In this stage there is a fast spread of micro-cracks, becoming more localised and leading to fibre breakage and, in the case of the cross-ply composites, also to delamination. The specimens reach complete failure at this point. The advantage of using embedded sensors is evident when comparing the number of acoustic events sensed by the surface mounted and embedded sensors. the specimen with surface mounted and embedded sensor measured, respectively, 35×10^3 and 30×10^4 acoustic events in total in the unidirectional specimens and 33×10^3 and 59×10^3 acoustic events in total in the cross-ply specimens. It was also observed that the unidirectional laminate with embedded piezoelectric sensor lasted for a slightly higher number of cycles than the laminate without embedded sensor, before breaking, while the cross-ply laminates reached rupture at the same number of cycles. Damage initiation locations and cracks in the laminates with embedded piezoelectric sensors were far from the sensors, showing that the sensors themselves did not promote damage initiation. Nevertheless, this study does not represent a real and large structural part, where, generally, a large number of sensors is used. A PZT sensor network covering large areas of a structural part requires lengthy and heavy cabling that may be harmful to its performance. Three approaches can be implemented to reduce the length of lead wires of PZT sensors network. The PZT sensors in the same row or column can be connected either in series, parallel or heterogeneous way, with a mixture of in series and parallel connection, to form a single continuous sensor. These strategies allowed to reduce the cabling length as opposed to if every single sensor of the network would have its own lead wire connected to a single channel of the monitoring system. These strategies were employed in a lightweight and low power consumption impact region monitor (IRM) system based on a PZT sensors network and guided waves and was validated on a composite wing box of an UAV, where the sensors were placed on the inner surface of the composite skin [43].

Piezoelectric wafer active sensors (PWAS) have also been exploited on SHM of aerospace composites with multipoint measurements, as they are inexpensive, of small size and require simple instrumentation. PWAS consist of an array of PZT disks or squares and can be both surface mounted on or embedded into the composite structure [44]. However, PWAS may present weak driving force/displacement, brittleness, and their use at high temperatures or under high strains/voltages may result in a non-linear response and hysteresis [14].

Commonly, two detection approaches are used with PWAS, electromechanical impedance (EMI) (standing Lamb waves), adequate for near-field damage detection, and propagating Lamb waves for far-field damage detection [44]. The EMI technique makes use of PZT transducers that under an electric field actuate and produce a harmonic force on the host structure, to stimulate a structural response, the electromechanical impedance (or admittance) "signature" [45]. Usually, the real part of impedance or admittance can be used for damage detection, while imaginary part of impedance or admittance can be used for detection of transducer debonding [46]. The electromechanical admittance signature is dependent on the length, width, thickness, and orientation of the PZT transducer, but also on the stiffness, mass, and damping of the host structure, allowing to sense structural damage, when changes on the impedance of PZT, $Z_E(\omega)$, are detected. The EMI can be measured by impedance analysers or LCR (Inductance L, Capacitance C, and Resistance R) meters [45]. This technique utilizes high-frequency structural excitations, typically higher than 30 kHz, with a sinusoidal source V_X, with angular frequency ω, to produce a current I. The electrical impedance of the PZT is presented in equation (4) [47].

$$Z_E(\omega) = \frac{V_X}{I} = \frac{1}{j\omega a}\left(\bar{\varepsilon}_{33}^{T} - \frac{Z(\omega)}{Z(\omega) + Z_a(\omega)} d_{3x}^2 \hat{y}_{xx}^{E}\right)^{-1} \tag{4}$$

where $Z_a(\omega)$ and $Z(\omega)$ are the mechanical impedances of the transducer and monitored structure, respectively, $\bar{\varepsilon}_{33}^{T}$ the dielectric constant, $\hat{y}_{xx}^{E}$ the Young's modulus, d_{3x}^2 the electric field constant, a the geometric constant and j the imaginary unit.

Some overall-statistics damage metrics were developed to evaluate the damage extent, through the differences on the admittance or impedance signature between the pristine and damaged state. Damage indexes, such as the root mean square deviation (RMSD) and cross correlation distance (CCD), are scalar numbers that give a metric of the damage in the structure. RMSD and CCD can be calculated following equations (5) and (6), respectively [48].

$$RMSD = \sum_{i=1}^{n} \sqrt{\frac{(R(i)_D - R(i)_R)^2}{R(i)_R^2}} \tag{5}$$

$$CCD = 1 - \sum_{i=1}^{n} \frac{\left[R(i)_R - \overline{R}_R\right]\left[R(i)_D - \overline{R}_D\right]}{\sigma_R \sigma_D} \tag{6}$$

where $R(i)_R$ and $R(i)_D$, at the i^{th} sample, are the resistances of the PZT transducer in reference and damaged state, respectively, $\overline{R}_R$ and $\overline{R}_D$ are the averaged values for reference and damaged state, respectively, and σ_R and σ_D are the standard deviations for the reference and damaged state, respectively. Although being simple and frequently used, the RMSD index is dependent on outside effects other than actual damage, such as temperature changes, as it shifts the impedance spectrum up and down [49].

Wandowski et al. [48] used electromechanical impedance technique to study delamination detection and localization in CFRP prepregs. The influence of temperature on the statistics damage metrics was evaluated as well. Delaminations of different sizes were induced through a chisel

Fig. 6. (a) SMART Layer strips embedded on bottle during filament winding process; (b) finished bottle. Adapted from [54].

that was hit in between layers of the sample. The samples were 100 × 100 × 3.5 mm in size and were evaluated in the frequency range between 1 and 50 kHz at four conditions, no damage at 22 °C, no damage at 24 °C, and two conditions with different size of delamination at 22 °C. The effect of temperature was observed as a vertical shift on the resistance characteristic and a small horizontal shift on the frequency. The RMSD index was calculated, where the sample without damage at 22 °C served as reference condition. The small increase in temperature of 2 °C produced a high value of RMSD, of about 700, showing high sensitivity of RMSD to temperature. Although the RMSD value for the sample with the smallest delamination, circa 1300, is higher than the RMSD value for the sample exposed for the small temperature change, it would be difficult to discern damage from a temperature variation in a real situation with a smaller delamination. The CCD value of the sample exposed to the temperature variation is much smaller than that of samples with delamination, being around 0.004, 0.04 e 0.06, for the sample without damage at 24 °C, and for samples with progressively larger delaminations, having as reference the sample without damage at 22 °C. The high RMSD value for the small temperature variation is due to its sensitivity to horizontal and vertical shifts of the spectrum, while the CCD index is only sensitive to horizontal shifts. With another set of samples, of dimensions 600 × 200 × 3.5 mm, the effect of temperature was further evaluated in the frequency band between 1 and 20 kHz, as damping effect was observed for higher frequencies, resulting in wide resonant peaks with low amplitude. It was observed that the resonant peaks are shifted in frequency for different temperatures, and those shifts are dependent on the frequency. For that, the authors propose an algorithm for temperature compensation based on cross correlation, where the CCD index is applied to narrow bands of frequency but covering the total analysed frequency band. Thomas and Khatibi [50] evaluated the integrity of surface mounted and embedded PWAS on carbon fibre/epoxy composites under repeated impact loading, resorting to electromechanical impedance and capacitance measurements. Both methods revealed the superior integrity of embedded PWAS. EMI analysis, generally, showed a higher RMSD for samples with surface mounted PWAS than samples with embedded PWAS. For instance, the RMSD of specimen with surface mounted PWAS was 6.51 after the 3rd impact with 7 J impact energy, while the RMSD of the specimen with embedded PWAS was 0.46 after the 9th impact with the same impact energy. The capacitance measurements of samples with embedded PWAS revealed that the sensors can survive various impact events of different energies, keeping the capacitance values between 1 and 1.05, except for impact energies of 10 J, where the sensor showed a capacitance of about 0.7 after the 9th impact event, revealing some extent of damage. Regarding surface mounted PWAS, an impact energy of 5 J produced a capacitance increase after the 3rd impact event, from 1 to about 1.05, associated with partial debonding, with subsequent decrease in the following events, reaching a capacitance of about 0.6 in the 9th event. The specimen with surface mounted PWAS subjected to an impact energy of 7 J had similar response and the specimen subject to an impact energy of 10 J reduced the capacitance to about 0.5 just after the 1st impact.

PWAS transducers can both receive and transmit Lamb waves through the composite structure, serving as both sensor and actuator, respectively, through in-plane strain coupling [14]. Lamb waves require simple instrumentation: a signal generator, a digitizing oscilloscope, and a PC [14,44]. As guided waves can propagate through long distances, few meters, it is possible to detect damage over a large area of a structure, using just a few transducers [51], allowing to detect structural anomalies, such as cracks, corrosions and delaminations in thin-wall structures [7], and to monitor even holes, notches and degradation of lap joints [51]. However, some disadvantages exist. Signal interpretation is very challenging as Lamb waves are dispersive and present simultaneously symmetric and anti-symmetric wave modes that overlap each other. Some approaches to discern a "clean'' single propagation mode are reported in the literature, by appropriately locating PZT, promoting interactions between different Lamb wave modes, resulting in their minimization or even elimination, and consequently, on the enhancement of a single propagation mode [51].

Piezoelectric powder and piezoceramic fibres incorporated into epoxy resin to form poled film sheets, known as piezocomposite transducers, have been developed to overcome the brittleness of traditional PZT sensor/arrays, but also enhancing sensor flexibility for surface conformability in curved structures. An example of a piezocomposite transducer is the macro fibre composite (MFC), developed by NASA back in 1992, for applications like structural control, vibration suppression and guided wave activation. The transducer is composed of unidirectional piezoceramic fibres, covered on both upper and lower surfaces by inter-digitated electrodes and protecting epoxy film [52]. While the activating motion of a traditional PZT sensor is across its thickness, the activating motion of a MFC is along its piezoceramic fibres, leading to a driving force that can be three times higher on MFC than on PZT [14].

Other flexible sensors are available on the market, such as the SMART Layer™ produced by Acellent Technologies, Inc. PWAS are connected by a printed conductive pattern on a thin flexible dielectric film for electrical insulation, that can be either embedded or surface attached on the composite. It is suitable for both metallic and composite structures and comes with an epoxy adhesive film on one side of the layer for convenient surface bonding. The SMART Layer™ embedment is done during manufacturing where the sensing system is placed as an extra ply. The SMART Layer™ can be co-cured with several composite materials, as it can sustain temperatures as high as 200 °C [53]. The use of the SMART Layer was even demonstrated to be adequate for impact damage detection and location on filament wound composite structures that could be employed on solid rocket motor cases and liquid fuel bottles [54]. Eight strips were embedded into a filament wound composite bottle with an aluminium liner, each strip having five PZT sensors of 6.35 mm diameter and 0.25 mm thickness. Four strips were embedded

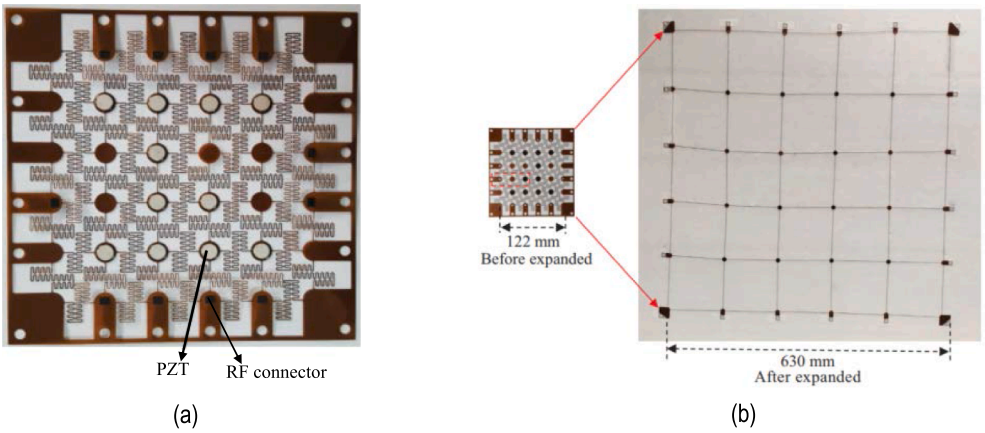

Fig. 7. (a) guided wave based sensor network with an effective area of 122 mm × 122 mm; (b) full expansion of the guided wave based sensor network to an area of 630 mm × 630 mm. Adapted from [55].

one layer above the liner and four strips one hoop layer below the surface of the bottle. The distance between two neighbouring PZT sensors was 140 mm on the cylindrical section and 114 mm on the dome section of the bottle, and 153 mm in hoop direction, producing a square grid of sensors spread over the bottle. Some of the stripes can be seen in Fig. 6, as well as the finished bottle. The diagnostic system forwards an electric signal to the PZT actuators, which consequently produce a stress wave that propagates through the structure, per converse piezoelectric effect. This mechanical excitation is detected by the PZT sensors, by piezoelectric effect. The health condition of the structure over time is assessed by using the diagnostic software that collects the sensor signals over time and compares them with a baseline signals set, following the Lamb wave approach. The difference between baseline and after impact damage signals produces a scatter signal, which can be used to locate and determine the extent of the produced damage. The scatter signals for all defined actuator-sensor paths can be processed to render an image that shows the location and size of the damage. An impact damage with an area of about 12 mm × 20 mm was successfully located by the diagnostic software.

Wang et al. [55] reported the development of a stretchable sensor network based on guided Lamb waves. The authors claim that the stretchability of the system allows scaling it up so that it can be applied on aircraft smart skins. The sensors were produced by flexible printed circuit process and consist of 11 PZT elements and 11 micro radio frequency (RF) connectors on a polyimide substrate with copper metalized serpentine-based fractal interconnects, produced by laser cutting, that are connected to the PZT elements and RF connectors, through reflow welding. The serpentine-based fractal interconnects can pass on the signals or bear the tensile deformation. The network has an effective area of 122 mm × 122 mm and thickness of 0.12 mm (Fig. 7 (a)), which can stretch up to an area of 630 mm × 630 mm (Fig. 7 (b)). The stretched sensor network was bonded to the surface of a carbon fibre composite laminate with stiffeners, of 1000 mm × 1000 mm × 3.4 mm, using epoxy adhesive. The sensor network system demonstrated to be suitable for the application of both active and passive guided wave sensing methodologies for impact monitoring. The time-of-flight of the signals was used to construct damage imaging that revealed to accurately locate impact damage positions. However, impact damage sensitivity cannot be evaluated as the impact energy was not mentioned in the paper.

Another alternative to traditional PZT are piezopolymers, such as PVDF or PVDC, offering lightweight, conformability and high voltage-generating piezo coefficient. However, PVDC is mainly found in sensing applications for the food packaging industry. Oppositely to PZT, PVDF has low stiffness and therefore low strain-generating piezo coefficient [7]. PVDF sensors can assume varied shapes. Jung and Chang [56] developed PVDF grid fabric sensors, where some carbon fibre tows were removed from dry carbon fibre fabrics and replaced by PVDF film stripes in a grid fashion. The grid is formed by two PVDF stripes laminated with conductive copper tape, of smaller width, in between, to prevent electrical contact between the carbon fibres and the copper electrode. The fabric sensors were embedded into carbon fibre/epoxy prepregs as a regular layer. Following frequency analysis of Lamb waves, different failure modes produced by low velocity drop-weight impact tests were discerned: matrix micro-cracks with frequencies between 50 and 170 kHz, with 170–220 kHz, fibre–matrix debonding with 220–300 kHz and fibre breakage with 300–500 kHz. The extent of accumulated damage from consecutive impact events was estimated resorting to a failure index. Lambinet and Khodaei [57] reported the successful detection of artificial damage on adhesively bonded patch repair on carbon fibre composite laminates through the use of ring shaped PVDF sensors. The presence of distinct damages was detected using EMI and Lamb wave analysis, although damage location was not identified.

This review shows how versatile PZT sensors are. PZT sensors can be used on their own or in arrays, or even assembled in flexible films, following multiple constructions, or stretchable grids. The direct piezoelectric effect and the converse piezoelectric effect allow that PZT transducers can be used in both passive and active sensing methodologies. While an active sensing approach can assess the structural condition of a part at any time, a passive sensing approach only provides information about damage as it occurs. The level of damage detection is highly dependent on the used sensing technique. Acoustic emission is a highly sensitive technique, but it requires the structure to be loaded to create an acoustic emission event. It can only detect damage that releases energy, such as translaminar cracks, fibre breakage, delamination, fibre–matrix debonding and matrix cracks, whereas a stable crack, not spreading, is not detectable. Electromechanical impedance is also very sensitive to damage, but can be affected by environmental factors, such as temperature. This technique can only assess the current state of a structure by comparison with a baseline condition and can only give indication of damage extent resorting to statistic metrics. Lamb waves can monitor large areas of a structure and are able to detect internal damages, such as cracks, delaminations, matrix cracks, fibre breakage and porosity, in thin structures, as well as impact damage. While it can perform well on flat laminates, its applicability on real structures of more complex shapes is still limited. Damage location is also possible. All these techniques require skilled technicians to accurately evaluate data and associate it to the exact type of damage.

3.2.1. *Piezo-resistive sensors*

Piezo-resistive materials respond with a change of electrical resistance when subject to a mechanical stress/strain [58]. Traditional commercially available piezo-resistive sensors are based on metallic

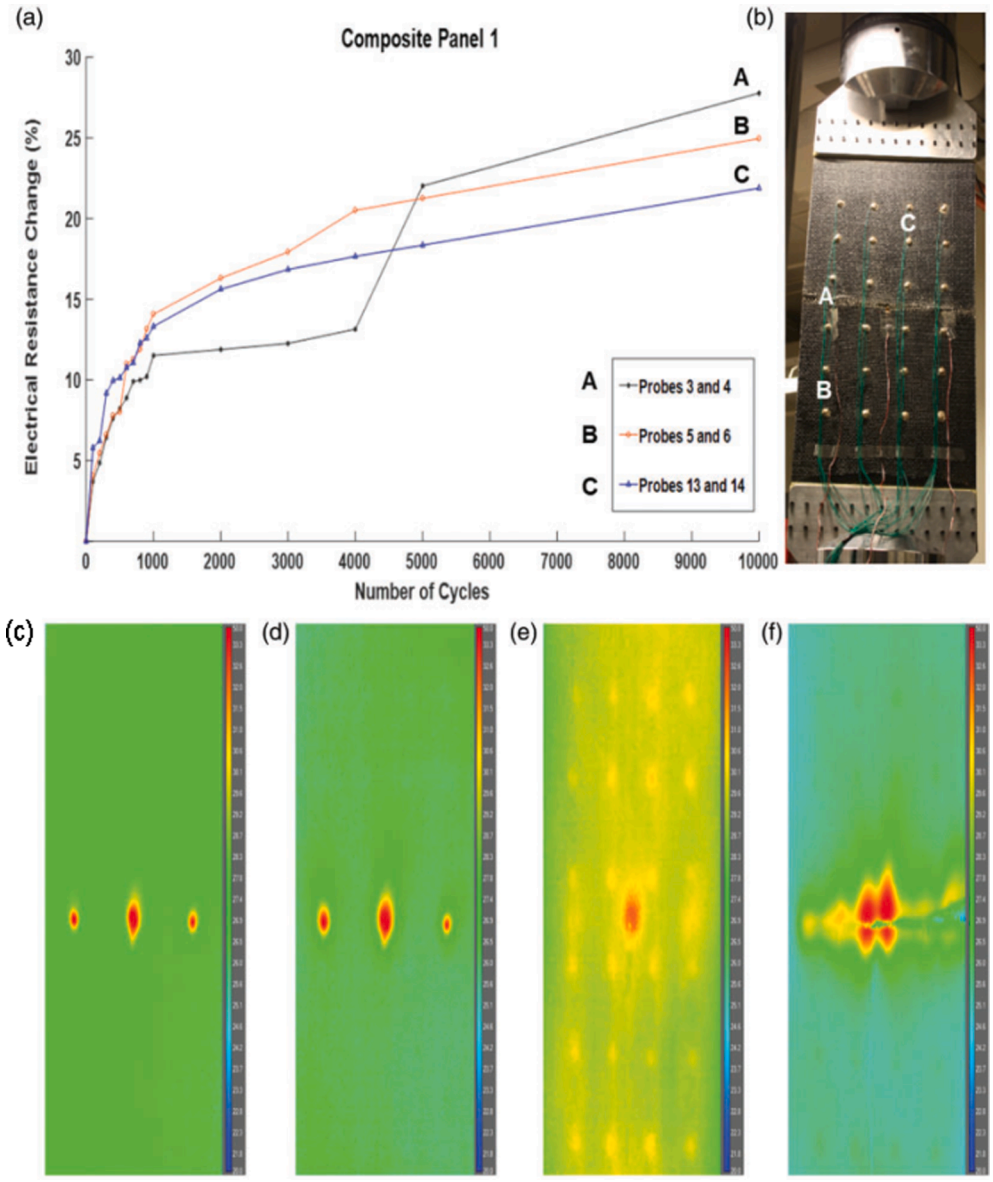

Fig. 8. (a) percentage of electrical resistance change on the locations with the highest variations during a cycling fatigue test; GFRP panel after failure; thermograms of the GFRP composite at different cycles: (c) 100, (d) 1000, (e) 10 000 and (f) right after fracture [75].

films that present poor flexibility and stretchability, or semiconductor materials that, even though they present great piezo-resistive sensitivity, they present reduced mechanical properties [59]. The use of carbon based materials, such as carbon fibres [60] and nanocarbon materials such as carbon nanotubes (CNT) [61], graphene [62–65] and graphite [66], might be a promising approach for sensing applications in SHM of aerospace composites. Furthermore, these nanocarbon materials may also introduce a reinforcing effect by improving the mechanical properties of the composite structure. While CF can be self-sensing, the nanocarbon materials can be incorporated in the FRP composites following different approaches, namely, nanocarbon reinforced matrix or nanocarbon in between prepreg layers, nanocarbon coated fabric, nanocarbon containing polymer film and nanocarbon coated fibre sensors, to take advantage of their piezo-resistive properties for sensing applications.

Carbon fibre reinforced composites can make use of a self-sensing approach, by utilizing the CF themselves as sensors to monitor damage by measuring induced changes in the intrinsic electrical conductivity of the fibres. This approach avoids introducing sensors in the CFRP, preventing the impairment of the mechanical properties of the host composite. Nevertheless, this approach is generally limited to damages involving fibre breakage, which usually happen as the part approaches the end of its service life, instead of detecting early damages that might happen in the resin, such as matrix cracks or debonding, that would allow for early preventive measures. A few recent studies [60,67–69] have demonstrated the applicability of electrical resistance tomography (ERT) for detection and localization of simple damages, such as drilled holes, drill rivets, superficial cuts, embedded razor blades, and local indentation, on CFRP composites. Several electrodes are installed on the CFRP boundary and current is injected through a pair of electrodes, while the resultant voltage is measured in the remainder boundary electrode pairs, allowing to construct a tomographic image of the conductive medium [70]. ERT is still at a low technology readiness level (TRL), as the electrical anisotropy of CFRP composites imposes a challenge for the reconstruction of tomographic images and due to its low spatial resolution [67].

To ease detection of early matrix related damage on CFRP, or on insulating glass fibre reinforced polymer (GFRP) composite, matrix

reinforcement or surface functionalization of reinforcing fibres with electrically conductive nanocarbon materials are valid solutions. CNT offer great properties that makes them a primary choice for reinforcement of matrix resins. The advantages of CNT are now well know, they do not only have great mechanical strength and high electric conductivity, but they also have high aspect ratio allowing to obtain a very low percolation threshold, at as low wt% as 0.1, without altering significantly the properties of the matrix resin [71]. When a crack spreads in the composite, the electric conductive percolating network of CNT will be disrupted, making the damage detectable by an increase in the electrical resistivity [72]. The resistance of the CNT network is dependent on the CNT intrinsic resistance and on the intertube resistance, which arises from the contact resistance between connected CNT, and from the electrical conduction in between CNT separated by sub nanoscale gaps, known as the tunnelling effect. Therefore, as CNT structure does not change with deformation, making the CNT intrinsic resistance insignificant, the resistance changes of nanocomposites due to deformation is attributed to the contact resistance in between connected CNT and to the changes in the tunnelling current. The tunnelling effect taking place at a sub nanoscale makes any small deformation likely detected [61]. A study reported by Zhang et al. [73] showed enhanced stability of the sensing signals by introducing CNT in between layers of CF prepregs, as the sensing mechanism was due to tunnelling current in the percolated network of CNT in the resin-rich areas, instead of physical contact among the conductive CFs of the prepreg material. Moriche et al. [63] evaluated graphene nanoplatelets (GNP) reinforced epoxy nanocomposites and multiscale GNP reinforced epoxy/GF composites, produced by hand lay-up. Initial GNP/epoxy nanocomposites allowed to find the percolation threshold at about 8 wt%, much higher than threshold values reported for CNT. Yet, the GFRP composites were produced with 12 wt% GNP on the epoxy matrix. Flexural test revealed that while the 12 wt% GNP/epoxy nanocomposite had improved properties when compared to the neat resin, the multiscale GNP - GFRP composite had inferior mechanical strength and strain at break than the GFRP composite. This is explained by the poor interface between the glass fibres and the GNP reinforced epoxy. GNP agglomerates lessen the interlaminar shear strength of the multiscale composite, easing delamination during flexural testing.

Some studies have shown the prospect of damage detection through nanocarbon material matrix reinforcement. Baltopoulos et al. [74] reported the use of ERT to create different regions of voltage distribution, in different parts of GFRP, by injecting current at different points of the CNT network, dispersed in matrix resin. A defect in the GFRP will produce a disturbance in the electrical path of the CNT network, which will be seen by the current source as a change on the total apparent resistance, and by the voltage meter as a change in the local current flow. The authors assume a CNT 3D fashion homogeneous network in the polymer matrix that allows monitoring several damage modes, drilled hole, notch and indentation, in the composite laminate. The low electric conductivity of the glass fibres and epoxy matrix allow to use very low current (10^{-5} A) capable of producing measurable voltage changes to detect damages, in contrast to previous studies on CFRP that required a higher current (0.1 A). A recent technique was proposed by Naghashpour et Hoa [75], with MWCNT reinforced epoxy for damage location assessment. GFRP composite laminates with 0.30 wt% MWCNT reinforced epoxy were produced by hand layup and autoclave curing. The laminates were about 813 × 356 × 1.9 mm and had a 24-point grid, separated by 76.2 mm, made of an electrically conductive paste of silver and epoxy, which was surface mounted on the GFRP panel. Electrodes were obtained by connecting electrical wires to the grid points. The behaviour of the panels was analysed in fatigue tests by monitoring their strain and electrical resistances and measuring their temperature distribution by infrared thermography. A broken GFRP panel, after a tension–tension cycling test, with an electrically conductive grid on its surface can be seen on Fig. 8 (b). Fig. 8 (a) shows the percentage of electrical resistance change on the locations with the highest variations, A, B and C as indicated on Fig. 8 (b). At first, location C presents the maximum electrical resistance change, being then overtaken by location B, until when, at about 4000 cycles, the percentage of electrical resistance change in location A started to increase, being where the final failure of the composite eventually occurred. Fig. 8 (c) to (f) shows the thermograms of the GFRP panel at different cycles, 100, 1000, 10 000 and right after fracture, respectively. The authors claimed that this study allows to experimentally monitor the random initial matrix cracking happening in the composite panels.

Sometimes the incorporation of CNT in the matrix resin might be difficult to homogenize and may lead to highly viscous resins, even at concentrations as low as 1.5 wt%, making the production of such composites by, for example, resin infusion, a challenging process. The use of CNT containing polymer film sensors may be a feasible alternative, although it may raise concerns regarding sensor fragility, weak van der Waals CNT/polymer bonding, and poor adhesion of the sensor to the host structure. Nag-Chowdhury et al. [20] reported the production of multi-walled carbon nanotube (MWCNT)/epoxy film sensors, produced by spray layer-by-layer (LbL) deposition technique, and their embedding into GFRP laminates during resin infusion. The authors stated that the sensitivity of the CNT based sensors could easily be adjusted by the content of CNT and number of deposited layers in the LbL process. During cyclic tensile tests, the electrical resistance of the embedded sensors followed the induced strain curve, for low values of strain in the elastic region, and came to zero after unloading of the first cycle. As soon as the plastic region was achieved, the sensors presented a residual

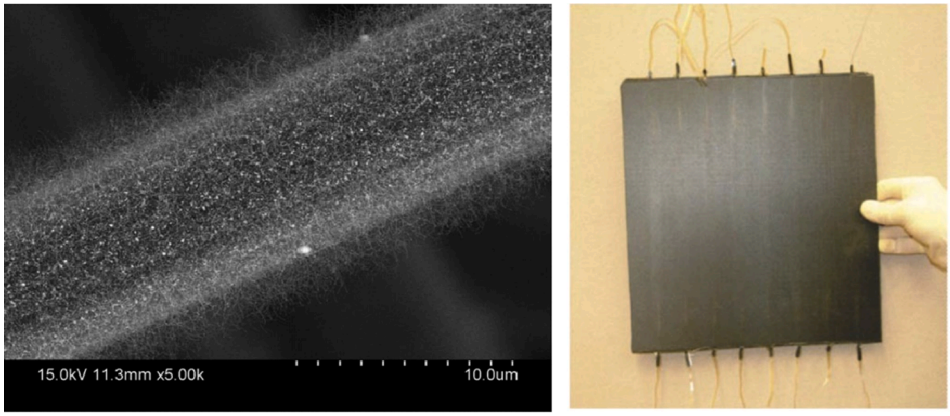

Fig. 9. (a) SEM micrograph of CNT grown on glass fibre for strain sensing and (b) carbon/epoxy composite panel with embedded sensors [78].

resistance after unloading of the second cycle, which can be explained by crack re-opening and new damage accumulation, allowing the sensors to monitor the residual strain accumulation. After five cycles, accumulated damage resulted in the rupture of the composite and sensor, with the disruption of the conductive percolated CNT network. Takeda and Narita [76] produced CFRP substrates and bonded them with a MWCNT based epoxy adhesive layer, where different MWCNT concentrations, between 0.32 and 1.3 wt%, were tested, to be used in aerospace structures. The specimens were subject to mode I loading for crack monitoring with a double cantilever beam, while the electrical resistance of the joint was being recorded with a digital ultrahigh resistance/micro current meter. Naturally, the increase on MWCNT content results in increased electrical conductivity, but the fracture toughness of the adhesive joint decreased for MWCNT at 0.65 wt%. The crack extension could be measured by the resistance change. Jan et al. [64] reported a graphene nanosheets/ thermoplastic polyurethane (TPU) composite film to be surface mounted on GF/epoxy composites produced by vacuum assisted resin infusion. The composite film had 12 wt% of graphene nanosheets, as this volume fraction showed an increased conductivity. A composite film strip of 3 cm × 0.25 cm was glued to the middle of the surface of each 300 cm × 25 cm composite specimen. The relative resistance measured by the graphene composite film was able to follow the amplitude of the imposed strain loading during cyclic tensile testing, though showing mechanical hysteresis as the relative resistance curve was drifting towards lower values, and some signal noise was also observed.

Another simple alternative approach to CNT reinforced resins is the use of CNT fibre [77] or CNT coated glass fibre sensors [78,79]. Alexopoulos et al. [77] embedded CNT fibres into GFRP produced by resin infusion without prejudice of the mechanical properties of the final laminate. The specimens were exposed to cyclic tensile tests and the applied loading and electrical resistance change on the CNT fibre were observed to be correlated in a parabolic way. Residual electrical resistance was observed for high values of applied loading, due to accumulated damage. Sebastian et al. [78] reported CVD grown CNT on top of glass fibres, to be used as sensors for SHM of CF/epoxy composites (Fig. 9). The fuzzy fibre sensors were electrically isolated in between two layers of plain weave E2 glass fibres and embedded in the midplane of the conductive composites. The reported system presented comparable sensitivity to conventional strain gages, with the advantages of being easily embedded into the composite and being able to sense a large area and at locations not easily read by strain gages. Another study conducted by Luo et al. [79] reported the embedment of single-walled carbon nanotube (SWCNT) spray coated glass fibre sensors into GFRP, for both process monitoring and in-service SHM. The SWCNT coated fibres were able to perform in-situ cure monitoring during the vacuum bagging production of the GFRP laminates, by revealing electrical resistance changes in accordance with the curing temperature program. At the strain-softening transition, the piezo-resistivity behaviour of fibre sensor systems switches from negative to positive, corresponding to micro-cracks opening and propagation in the epoxy matrix and fibre delaminations, depicted by an increase in the electrical resistance of the sensors due to the disruption of the conductive CNT network. The sensor was able to detect composite failure, which happened at a large strain of 5.1%, allowing to perform SHM with early detection of micro-cracks, preventing catastrophic failures.

Similar outcomes can be attained using graphene and graphite. Many works report the production of sensors consisting of graphene/ graphite coated fibres, mainly but not only limited to glass fibres, as reported in the following works [62,66,76,80]. Luo and Liu [66] have reported the production of a graphite nanoplatelet spray coated single filament glass fibre sensor, obtained by an aqueous dispersion of graphite nanoplatelets and a surfactant agent, following a drying, washing, and ambient drying process. The graphite nanoplatelet sensor was embedded in GFRP laminates produced by vacuum bagging of 0°/90° E–glass prepreg. Piezo-resistivity was measured during cyclic tensile testing on a dynamic mechanical analyser (DMA), allowing to calculate the gauge factor of the sensor, which revealed to be 17, although it became only 2.42 when embedded in the GFRP laminate. Piezo-resistivity measurements during fatigue tensile testing on the DMA were also used to verify the longevity of the sensor for SHM of composites. A tensile testing was taken to failure to demonstrate the ability of the sensor to detect damage. During the initial elastic deformation, the sensor increases its resistivity linearly, and when the composite enters plastic deformation, the resistivity continues to decrease but at a lower rate. As the composite reaches failure, resistivity increases drastically. Additionally, the sensor was able to monitor the 2-stage curing process during production of the laminates, which is discussed in Section 4.1. The authors claim that the developed sensor can be easily embedded on composites of more complex shapes at any required location and orientation in a non-invasive way, thanks to its continuous form. Nevertheless, further research work is required in order to make the sensors suitable for conductive composite materials, such as CFRP. It should be pointed that the reported work has used very small sample sizes. Balaji and Sasikumar [62] have reported the use and embedment of a reduced graphene oxide coated glass fibre sensor for real-time strain monitoring, as well as residual strength and damage accumulation estimation based on statistical analysis, on GFRP composites during uniaxial tensile testing. The sensor showed a linear piezoresistance with strain and applied force in low strains up to 3.7% (elastic region), explained by the tunnelling effect and an effective conduction path. For higher strains, the sensor showed nonlinear response, with step increments, explained by the breakdown of the conductive path as micro-cracks spread in the composite. The divergence of piezoresistance from the elastic behaviour was used to statistically estimate damage accumulation and residual strength of the GFRP composite. Upon failure of the specimen, either by fibre pull-out or matrix failure, the reduced graphene oxide-based sensor showed a sharp increase of piezoresistance, but further work is needed to associate the failure mechanism with the piezoresistance change. Montazerian et al. [65] reported the production of a graphene-coated spandex fibre sensor with a protective stretchable silicone sheath for monitoring the hot press manufacturing of GF/ polypropylene (PP) prepreg composites. The sensors were embedded in the midplane of 2 and 4-ply laminates and their suitability for SHM was assessed by three-point bending testing with imposed

Table 2
Comparison of the different sensing approaches using nanocarbon materials and self-sensing carbon fibre composites.

Sensing Technique	Advantages	Disadvantages	Damage detection
Self-sensing composite	No need for sensors	Limited to close to failure damage detection, limited to conductive fibre composites, mainly limited to flat or almost flat samples	fibre breakage, damage location using electrical resistance tomography at low TRL
Nanocarbon material matrix reinforcement	Percolation at low volume percentages for CNT	Difficult composite processing	Detection of early matrix dominated failure modes, damage location assessment possible
Fibre/fabric coating	Easy processing	Cannot assess damage location and size, limited to insulating fibre reinforced composites	Detection of early matrix dominated failure modes
Film sensor	Applicable to both insulating and conductive fibre composites	Poor adhesion bonding of sensor to host structure, fragile	Elastic strain, residual strain, and rupture by relative resistance change

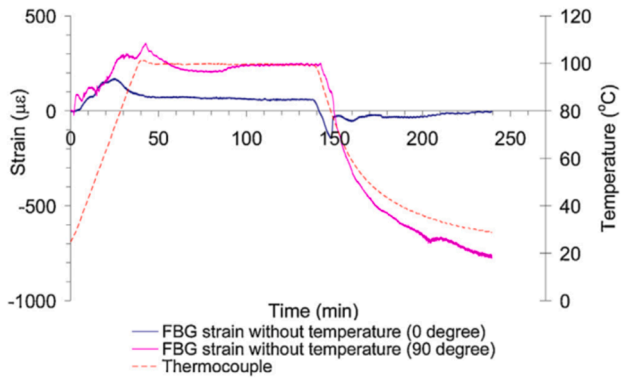

Fig. 10. Strain monitoring during cure reaction of a prepreg laminate [35].

increasing strain amplitude. The sensors could follow the variation in the elastic strain amplitude, measure a change in the residual resistance in the fourth and fifth cycles, due to progressive failure with imposed loading, and identify failure fracture with the disruption of the conductive fibre sensor.

Table 2 summarizes the main advantages, disadvantages and damage detection accomplishments with the above described methods using carbon based sensing approaches. Scaling up laboratory specimen to real large-scale structures and understanding and attributing sensing signals to specific failure modes of composites is still very challenging. Some research work, though still at a low TRL, have shown promising results towards damage location, through CNT reinforced matrix. The low percolation thresholds attained with CNT, compared to graphene and graphite, make this the most favourable nanocarbon reinforcing material for piezoresistive sensing, easing composite processing, and minimizing nanocarbon material agglomeration.

4. In-situ process monitoring

Cure and process monitoring may provide the knowledge to keep up with the increasing demand for advanced FRP composites in aerospace industry, with ever desired improved performance and reliability. Often, sensors used for structural health monitoring of aerospace composites can be taken advantage of, to firstly use them for monitoring of the processing procedure of polymer composites, which can also be beneficial for quality assurance.

4.1. Cure monitoring

During production of thick structural FRP for load bearing applications, uniform curing throughout the thickness of the part should be attained to produce high quality parts and reduce scraping volumes and consequently decrease costs. By monitoring the cure reaction, the electric power can be adjusted, which helps optimizing processing time, reducing costs, and avoiding thermal degradation once the curing exothermal reaction may be auto–accelerated. Very distinct sensing approaches for cure monitoring of composites are discussed in the following paragraphs.

Strain measurements by FBG sensors can also be used for cure monitoring. The strain can be associated with thermal expansion at the time that the resin is heated, followed by a negative strain due to polymerization shrinkage as the resin starts to cure, and finally, higher negative strain may be developed as further shrinkage happens upon cooling. An optical fibre which is placed in a transverse direction to the reinforcing fibres will measure high compressive strains, since the matrix pays a large contribution to the properties of the transverse direction, while the strain is lower in the same direction of the reinforcing fibres. A study published by Boateng [35] followed the strain development during the curing procedure of prepreg laminates, involving a heating stage, isothermal curing period at 100 °C for 100 min, and cooling stage, using bare and encapsulated FBG sensors (Fig. 10). The data acquired by the encapsulated FBG sensors was taken to find the mechanical strain imposed in the FBG sensors during the cure reaction. At the end of the isothermal period, the strain values were about 220 and 60 με, as measured by an FBG sensor embedded in a perpendicular direction and by an FBG sensor embedded parallelly to the reinforcing fibres, respectively, while at the end of the cooling stage, the same sensors measure strain values of about −760 and close to zero με, respectively. As the temperature increases in the heating stage, a strain increase is recorded in both sensors due to thermal expansion suffered by the resin, though this effect is more pronounced on the FBG embedded perpendicularly to the reinforcing fibres. Initiation of chemical shrinkage due to polymerization is observed at around 25 min in the FBG sensor embedded parallelly to the reinforcing fibres, while it is unclear whether it starts at 30 or 42 min in the FBG sensor embedded perpendicularly to the reinforcing fibres.

Chilles et al. [6] proposed the embedment of inductively coupled piezoelectric sensors on glass fibre reinforced epoxy prepreg for cure monitoring and further damage detection. The sensor system consisted of a piezoelectric transducer electronically connected to an inductance

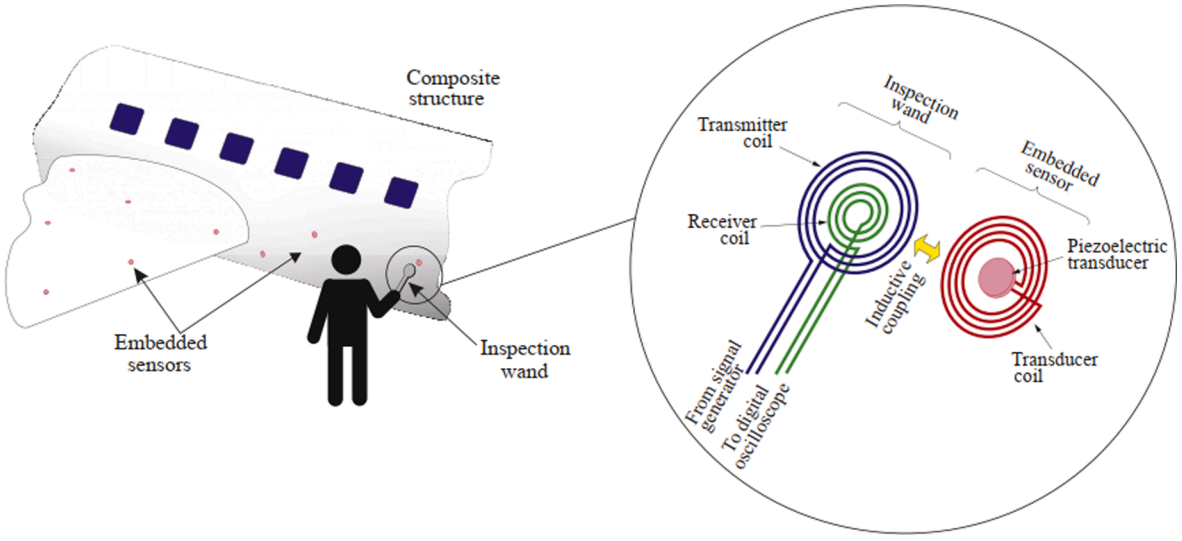

Fig. 11. Composite structure being manually inspected with an inspecting device, schematically represented on the right side, by the inductive coupling between the transducer coil in the piezoelectric transducer and transmitting and receiving coils in the inspecting device [6].

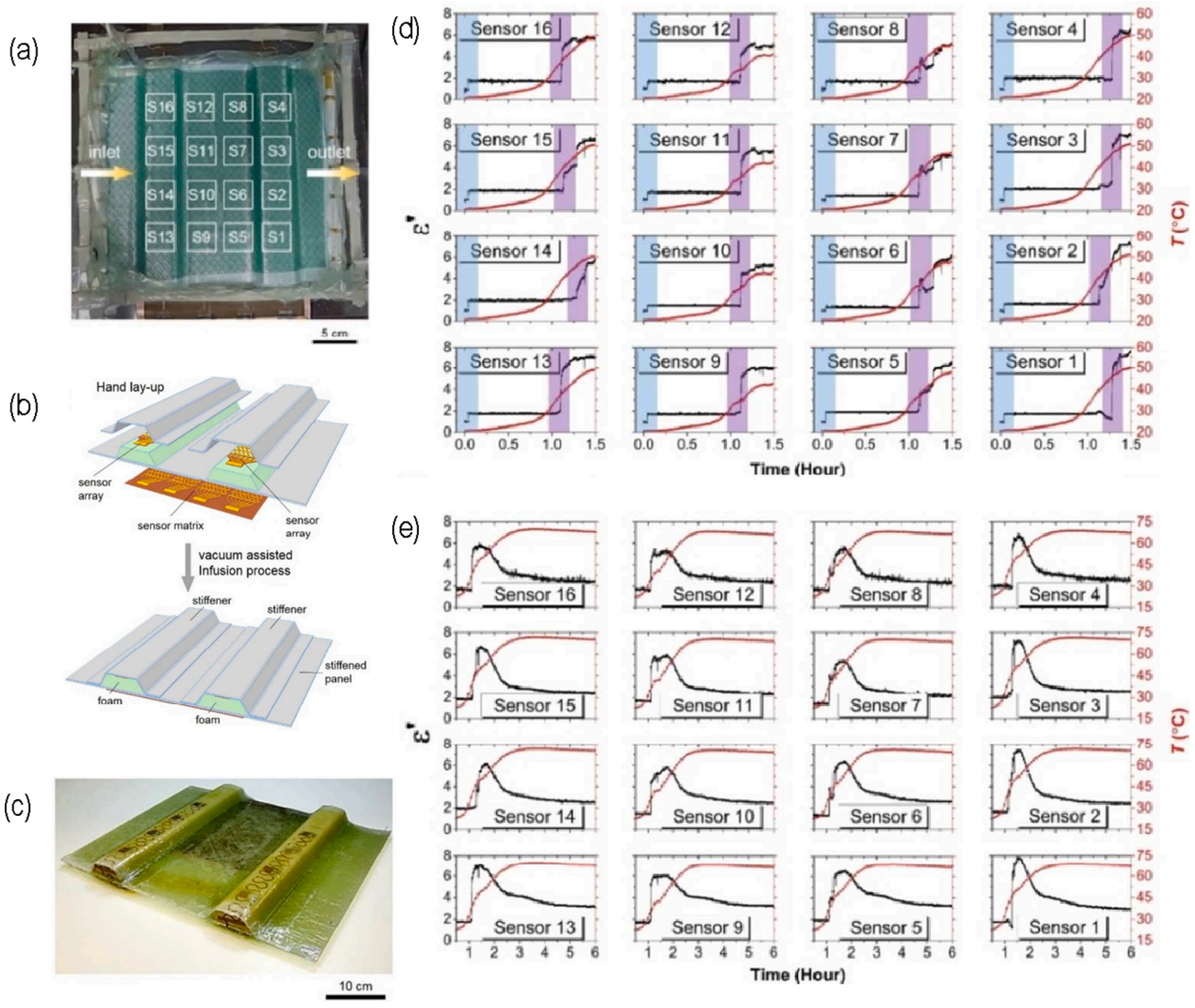

Fig. 12. Vacuum infusion process monitoring of a stiffened glass fibre reinforced epoxy composite: (a) top view photograph of the experimental setup with sensor locations representation; (b) schematic representation of the flexible sensors integration in the stiffened polymer composites (c) photograph of the produced composite with embedded flexible sensors; dielectric constant measurements at the (d) preparation and resin infusion stage and during the (e) cure reaction stage. Adapted from [83].

coil, and an inspection device containing a transmitting and a receiving coil, which are connected to the input and output of an ultrasonic instrumentation, allowing wireless communication (Fig. 11). A bulk wave generating system was used to monitor 10.4 mm thick composite plates and a guided elastic wave generating system was used to monitor thinner composite plates, with a thickness of 3.31 mm. The initial curing phase of the thick sample could not be characterized due to the low viscosity of the resin at this stage, while the embedded sensor using the guided wave system detected the edge reflections prior to initiation of the curing reaction, as the guided waves propagated along the fibres. The temperature increase led to the reduction of the resin viscosity, increasing the attenuation of the guided ultrasonic waves until they were no longer detectable. As curing progressed, the edge reflections became again detectable. Both systems proved to be suitable for the last phase of cure monitoring. Dielectric analyses were employed for comparison. The measurement of the imaginary impedance maximum was only possible when the dielectric sensor became wet by the resin. With the increase of temperature and decrease of resin viscosity, the imaginary impedance maximum decreased. The imaginary impedance maximum increased with the progression of the curing reaction. A steep increase due to the sudden decrease of ionic mobility during cure revealed resin gelation. The end of cure is identified by a constant value of the imaginary impedance maximum. Commercial dielectric analysers, such as the DEA 288 Ionic from Netzsch, enables cure monitoring in both laboratory and industrial scales, making use of implantable or reusable dielectric sensors. The reusable sensors can be even indefinitely mounted on a press or mould surface. The sample is placed in contact with the dielectric sensor. The sinusoidal voltage is applied forcing the positively charged particles in the sample to move towards the negative pole and vice versa, and dipole molecules are aligned, producing a sinusoidal current with a phase shift. As curing progresses, the sample viscosity increases and, consequently, the mobility of the charge carriers decreases, expressed by a decrease of amplitude and increase of phase shift in the current signal [81]. Though, the use of dielectric sensors and analysers is limited to cure monitoring and cannot be used for damage monitoring.

Luo and Liu [66] have reported the production of a piezo-resistive sensor consisting of graphite nanoplatelet coated single filament glass fibre sensor, already described in Section 3.3, and its use for cure monitoring. The sensor was embedded in GFRP prepreg laminates and was able to monitor the 2-stage cure of the vacuum bagging process. The sensor showed a steep increase of the resistivity, from 199.7 kΩ to 572.1 kΩ, as the temperature was increased from ambient temperature to 143 °C, due to the physical and chemical changes of the matrix. As the

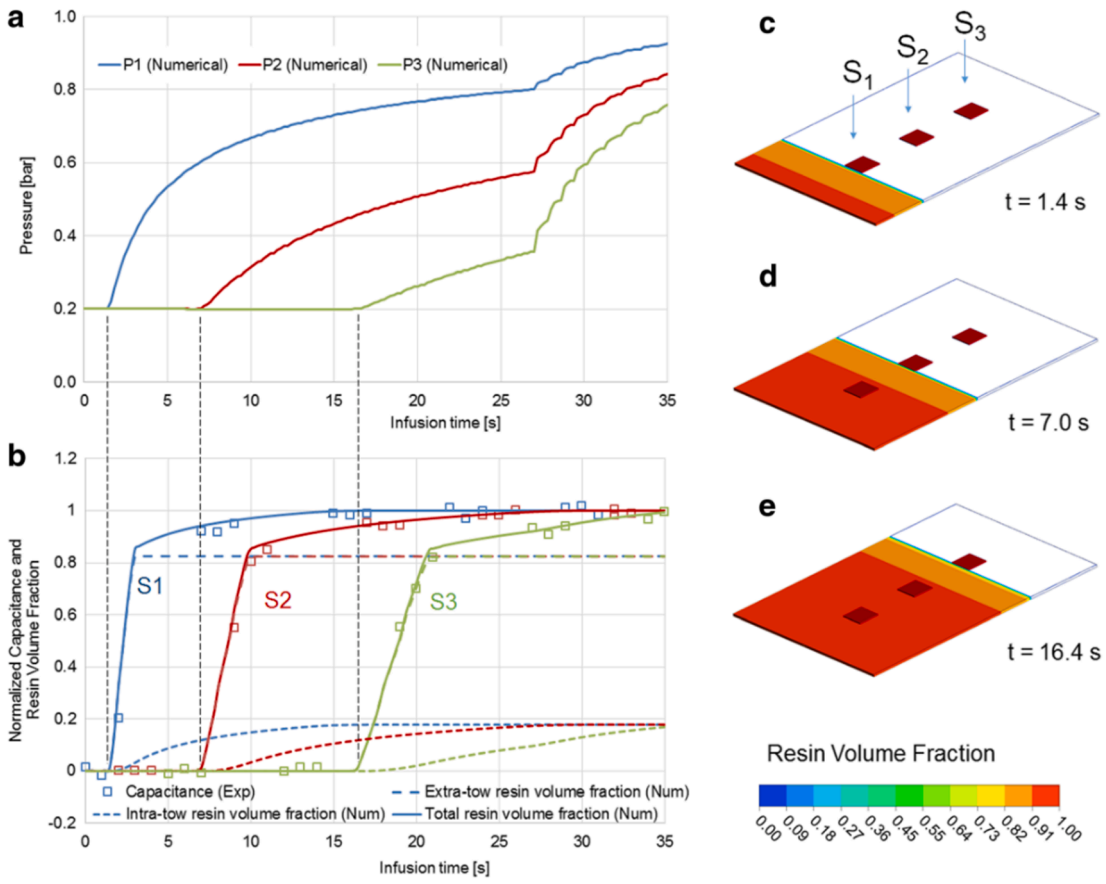

Fig. 13. numerical and experimental dada of a resin infusion process for the production of a glass fibre/polyester resin composite: (a) pressure profiles; (b) numerical and experimental normalized capacitance; and resin volume fraction and position plots at the initial detection by dielectric sensors (c) S1, (d) S2, and (e) S3 at different positions of the preform [85].

temperature increased, the viscosity of the resin decreased which makes it easier for the resin to fill in the gaps in between the graphite nanoplatelet particles at the fibre sensor surface and their contact to be further distant or disrupted and, consequently, induce an increase of the sensor resistance. The temperature ramp is followed by an isothermal stage, where cross-linking bonds further occur leading to the increase of resin viscosity and shrinking. During this stage, the resistance of the sensor decreased initially, from 572.1 kΩ to 466.1 kΩ, and was kept constant for the remainder isothermal period, with a value of 403.6 kΩ, which was explained by the interparticle graphite nanoplatelet contacts being closer together again.

The analysed sensing approaches were able to identify the completion of the cure reaction, generally by a plateau of the measured parameter, leading to enhanced properties of the composite. Although the reviewed sensing approaches are able to identify all the curing stages of composites, optical fibre sensors, namely FBG sensors, can evaluate the residual strain resulting from the matrix shrinkage due to curing happening in the isothermal and the cooling down period. This is a valuable information that can be useful to find the best curing cycle for certain aerospace parts where precise processing control is necessary to comply with demanding dimensional accuracy requirements.

4.2. *Mould filling in liquid composite moulding processes*

Distinct sensing approaches, including the ones discussed in the previous section, have been shown to be suitable for mould filling and flow front monitoring on the production of polymer composites through LCM techniques. Ali et al. [82] developed a sensing technique based on the piezo-resistive properties of a reduced graphene oxide thin coating applied on glass fabrics for flow front monitoring in the resin infusion process. The proposed sensing technique was able to monitor the resin infusion process of an epoxy resin. As the infusion began there was a sudden decrease of relative resistance, and as the resin flow progressed the resistance started to increase, due to the spring-back effect of the preform caused by the resin pressure gradient, which makes up for the dielectric properties of the resin flowing in. When the preform is fully impregnated and the injection line is closed, the resistance decreases until the pressure equilibrates. When the pressure settles, the curing starts and the resistance starts to increase, due to the insulating layers of cured resin around the fibres. This sensing technique may provide valuable information for LCM manufacturing methods, especially for techniques involving two closed rigid mould tools, such as RTM. The graphene coating provided insights about the compaction condition of the reinforcements, flow front progression and cure reaction as well, due to changes in the electrical resistance of the fabric. Yang et al. [83] produced flexible sensors by photolithography on polyimide-copper film substrate and with integrated temperature sensors, able to make simultaneous measurements of both capacitance and temperature. The sensors were employed for the resin infusion process of stiffened glass fibre reinforced epoxy composites (Fig. 12 (a), (b) and (c)). The sensors were able to monitor the vacuum seal, shown by an increase of dielectric constant ε' from 1 to 2, as the vacuum imposed a tighter contact between the sensors and glass fibres (blue shade in Fig. 12 (d)) and, one hour later, the resin flow front, identified by the sudden increase of ε' from 2 to around 6 or 8 as the resin flowed in and the air in between fibres was replaced by liquid resin (purple shade in Fig. 12 (d)). In the following curing time ε' was kept approximately constant, apart from sensors 6 and 8 where the ε' variation indicated a vacuum leak. Additionally, the system was able to monitor the curing rate by the rate of change of the dielectric constant ε', the progression of the internal temperature, and

resin vitrification (Fig. 12 (e)). While the authors claim that the sensors are capable of detecting delamination during SHM, it is unclear whether the sensors themselves are responsible for promoting this type of damage in the first place.

Alternatively, the sensors can be applied on the moulding surface tool and reused for several cycles. Carlone and Palazzo [84] reported the use of shielded dielectric sensors on the bottom die in contact with the preform to monitor the flow front progression in LCM process, where glass fibre weave was used as reinforcement and synthetic oil as resin replacement to prevent variations on the dielectric properties due to cure. The proposed sensing approach was combined with numerical simulations and were able to monitor both unsaturated flow front (flow developed in between tows, regarded as extra-tow flow, leading to the preform impregnation) and saturated flow front (flow developed inside each tow, regarded as the intra-tow flow, leading to the preform saturation). For reduced void content the fluid/resin should be able to fill and saturate the preform, whereas there is usually a short period of time between the unsaturated and saturated flow front. The sensors were able to detect the arrival of the fluid in the sensing area by a sharp increase of capacitance, and measure the arrival time, and to detect the time of full saturation in that same area, when the capacitance was no longer varying. Carlone et al. [85] have used the concept of capacitance variation as a sensing approach. Each dielectric sensor consisted of two flat electrodes placed on the bottom and top mould surfaces parallelly, to form a capacitor, where the central insulating material is the reinforcing glass fibres, polyester resin, and air in between the moulding surfaces. The extra-tow flow front progression was numerically modelled by bulk permeability simulations and was experimentally shown by the progressively increased time of arrival on the three sensors installed on the mould surfaces. The saturation rate was also computed, which allowed to find a good agreement between the experimental and numerical (sum of intra-tow flow and extra-tow flow) normalized capacitance data. The experimental and numerical data of an experiment is presented in Fig. 13.

Only a limited number of research works address the mould filing monitoring in electrically conductive carbon fibre–based composites. Qing et al. [86] exploited the concept of the SMART Layer™, addressed in Section 3.2, and employed a PZT sensor network on a flexible polyimide substrate with a printed circuit to connect the PZT sensors. The resin flow path could be followed by measuring the first arriving Lamb waves signals in between different pairs of PZT transducers. As the sensing path becomes wet by the resin, higher energy attenuation of the Lamb waves is measured, until the signal stabilizes at a low amplitude value when the preform is fully filled. It was also possible to follow the curing reaction. A study carried out by Wang et al. [87] monitored resin infusion processing of composite laminates made of unidirectional carbon fibre fabric arranged in 0 and 90° directions and epoxy. Fresnel's optical fibre sensors monitored the refractive index of the resin during impregnation and curing to evaluate flow front progression and cure reaction. Type-K micro-thermocouples were used for temperature reading. A combination of these two sensors in the midplane of the laminate allowed to distinguish five stages of the process. In stage 1, the infusion stage, it is observable the resin arrival by a sudden decrease on the OF signal as the reflected light is decreased by the presence of the resin around the sensor, and through a temperature minimum. In stage 2 there is a temperature increase. The curing stage corresponds to stage 3, with a 2 h isothermal at 180 °C. At the beginning of this stage there was a temperature peak, accompanied by an increase in the reflected light intensity, due to an increase on the resin density, as it changed from liquid to solid in the exothermal curing reaction. The resin was considered cured when there were no further changes on reflected light intensity. Upon cooling, stage 4, the resin shrinks, and its density increases, resulting in higher reflected light intensity. In stage 5, corresponding to the end of the resin infusion process, there is a stabilization of the temperature and reflected light intensity. A dielectric sensor [88] consisting of two twisted copper wires, each coated with an insulating material, to impede contact between copper and reinforcing carbon fibres, is able to monitor the flow front progression and cure reaction in the RTM process. A voltage is applied to produce an electric field between the wires, which goes through the gaps between the wires. The authors were able to calculate the flow front position, i.e., the instantaneous length of wetted sensor, by the linear admittance measured by the sensor. However, this concept can only be applied after the experimental calculation of admittance of the sensor in the dry and wetted condition, provided that the same reinforcement layup configuration and pressure profile in the impregnation stage is used. This can be a limiting issue in the production of a small number of high end large composite parts, where large material scraping, and increased costs could result.

5. Structural health monitoring systems for aerospace composites

A complete structural health monitoring system comprises not only sensors, but also a data acquisition system, data storage hardware and algorithms for signal processing, thus, involving interdisciplinary engineering fields. Having lightweight, compact, and low power consumption solutions are of foremost importance when designing SHM systems for aerospace applications. Although out of the scope of this review, a few considerations that should be regarded when conceptualizing structural health monitoring systems for aerospace composites are briefly presented in this section.

The choice between active and passive sensing systems should be considered when designing lightweight SHM systems. With an active sensing system, the monitored host structure is excited by actuators and the structural response is read by the sensors. The location and number of transducers must be adjusted to improve damage detection accuracy, keeping the associated weight and expenses low. However, an active SHM system bring the disadvantage of requiring an extra component, a signal generating hardware for excitation of the host structure, increasing power consumption and complexity of the system. On the contrary, for passive sensing systems, only sensors are needed to continuously monitor the host structure condition. But, while continuous monitoring ensures that damage is detected instantaneously, energy expenditure is maintained even when impacts are not frequent [89].

Wireless sensing systems can reduce the amount of cabling, wiring and electronics, an important advantage for the aerospace industry, which is constantly seeking weight reduction. Furthermore, the use of wireless sensing systems, following the IoT (internet of things) principle, in locations of difficult access in an aircraft may prevent difficult installations and maintenances, decreasing cost [89]. Power requirement is in the sub-mW range, enabling the use of batteries in such IoT systems [90]. Moreover, power requirements can be reduced using dynamic power management strategies, where the wireless sensing systems are configured to turn power on or off as needed, helps to reduce power consumption [91]. However, the accuracy of wireless data communication between the wireless sensor nodes acquiring data and the computing systems is compromised, due to lack of synchronization. The main research works to overcome synchronization discrepancies focuses on computing algorithms and on the use of GPS transceivers [92].

Energy harvesting systems bring promise to further develop wireless sensing systems, decreasing the overall weight of the system, and improving its autonomy. Energy harvesting systems make use of self-powered devices that take advantage of the numerous energy sources available in aircraft structures, needed to replace batteries of heavier weight. Examples of such energy sources are temperature differences, temperature changes, vibrations, strain, ambient light, pressure changes and electrostatic charges, being thermal and vibrational energy sources the ones that can produce harvesting systems with higher reliability and performance. The vibrational energy can be exploited by micro-generators driven by electromagnetic or piezoelectric conversion, and

Table 3
Characteristics comparison of different types of sensors for structural health monitoring for aerospace applications.

Type of sensor	Advantages	Disadvantages	Sensing Technique	Damage detection
Fibre Optic	Immune to electromagnetic interference, small size, light weight, cheap, durable, allow sensor multiplexing, sensing of large area structures, applicable to all type of composite materials, commercial solutions available solutions that can be tailored for each application	Expensive optoelectronic interrogation systems, temperature sensitive, fragility of the sensors makes embedding procedure challenging, strain is partially absorbed by the protective layer	Measurements of intensity, wavelength, phase change or state of polarization	Strain, low velocity impact damage, cure monitoring
Piezoelectric	high mechanical strength, operational for a wide frequency range, cheap, small sizes, work in both active and passive sensing methods, many commercial solutions available	Lengthy cables, difficult signal interpretation	EMI, acoustic waves, or Lamb waves	EMI: damage extent with statistic damage metrics; Lamb waves: detection of cracks, corrosion, delamination, holes, notches, degradation of lap joints, sensitive to small damages, can inspect large areas, can locate damage; Acoustic emission: passive sensing method, detection of matrix cracking, fibre–matrix debonding, delamination, fibre breakage, location of damage possible by triangulation
Piezo-resistive	Minimal structural intrusion of the sensor, mechanical reinforcing effect using nanocarbon materials, high damage sensitivity	Mainly limited to insulating composite materials	Electrical Resistance change, acoustic emission	Limited location of damage, early damage detection possible

the thermal energy by Seebeck effect. Yet it is still very challenging to produce devices capable of gathering sufficient energy to supply the wireless system [93].

6. Conclusions

The development and implementation of SHM systems requires the engagement of a multidisciplinary team to evaluate each specific case. The best sensing approach can only be chosen once analysed the specificity of the structure, including shape, size, constituent materials, loading condition and production technology, the operational environment, expected damage location and type and maintenance. Sensor location at strategic sites of the structure should be optimized to better detect damage. Even though it is possible to predict the locations prone to fatigue and corrosion cracking due to high mechanical loads and environmental conditions, unpredictable and random impact events may challenge the design of the sensor network. Not all types of sensors are suitable for carbon fibre composites. While FOS and piezoelectric sensors can be embedded in both GFRP and CFRP, a piezo-resistive approach may work best in GFRP, except if the carbon fibres themselves are used as sensors. While surface mounted sensors are more convenient to attach, maintain and replace, their accuracy might be affected by ambient noise as the sensors are directly exposed to the environment. Oppositely, embedded sensors have higher sensitivity, signal-to-noise-ratio, stability, durability, and repeatability, as they are protected from the environment. However, embedded sensors may face high pressures and temperatures during composite manufacturing, leading to short-circuits in the sensor system. It should also be considered that embedding a large number of sensors and wires may prejudice the mechanical properties of the host structure.

An effective structural health monitoring system must be able to detect early matrix related damage such as matrix cracks and debonding, allowing to take early preventive measures upon need. The analysed literature shows that fibre optic sensors, in particular FBG sensors, are able to detect subtle damages produced by low velocity impact events. The sensing techniques commonly used with piezoelectric sensors, electromechanical impedance, Lamb waves and acoustic emission, are all sensitive to damage, where damage identification and location is attainable through Lamb waves and acoustic emission. Within the wide range of piezo-resistive sensors, nanocarbon matrix reinforcement and fibre coated based sensors, and film sensors can detect early matrix dominated damage. While fibre optic sensor and piezoelectric sensors have been long researched, nanocarbon based piezo-resistive sensors are encouraging sensing approaches that may bring the advantage of mechanical reinforcing effect, as opposed to remainder types of sensors that may hinder the mechanical properties in the structure. Attending the aerospace environment, with unexpected impact events, for the reported sensing technologies to be fully adopted and widely accepted for structural health monitoring, more testing is needed on real scale composite structures.

Many sensors can be taken advantage of from the beginning of the production process and embedding procedure for cure monitoring purposes. Understanding sensor/host material interaction is fundamental to select a suitable location of the embedded sensors for cure monitoring. For instance, embedding FOS in the transverse direction of the reinforcing fibres can be advantageous for resin cure monitoring as the resin gives a high contribution to the transverse direction and produces higher compressive strain, as opposed to the longitudinal direction where the composite properties are mainly affected by the reinforcing fibres. However, the embedment of FOS in the longitudinal direction along the reinforcing fibres produces the least impairment of the mechanical properties of the host composite structure.

This paper is a review of the most relevant commercially available and laboratory made sensors for process and structural health monitoring of aerospace composites. Their sensing principles, characteristics, embedding procedures and interactions with host material were examined. An overall comparison and summary of the sensor types reviewed in the present paper is presented in Table 3.

Declaration of Competing Interest

The authors declare that they have no known competing financial interests or personal relationships that could have appeared to influence the work reported in this paper.

Acknowledgements

The authors acknowledge the support of the European Regional Development Fund [grant number NORTE-01-0145-FEDER-000015]; and of the European Space Agency through the Network/Partnering Initiative Program.

References

[1] Giurgiutiu V. Introduction. In: Structural Health Monitoring of Aerospace Composites. USA: Elsevier; 2016. p. 1–23.
[2] Holmes M. Aerospace looks to composites for solutions. Reinf Plast 2017;61(4):237–41.
[3] Ramakrishnan M, Rajan G, Semenova Y, Farrell G. Overview of fiber optic sensor technologies for strain/temperature sensing applications in composite materials. Sensors 2016;16(1):99.
[4] Giurgiutiu V. Shm of aerospace composites – challenges and opportunities. CAMX Conf ProceedingsProceedings 2015:1–15.
[5] Boller C. Next generation structural health monitoring and its integration into aircraft design. Int J Syst Sci 2010;31(11):1333–49.
[6] Chilles JS, Koutsomitopoulou AF, Croxford AJ, Bond IP. Monitoring cure and detecting damage in composites with inductively coupled embedded sensors. Compos Sci Technol 2016;134:81–8.
[7] Giurgiutiu V. Smart Materials and Health Monitoring of Composites. Elsevier Ltd.; 2017.
[8] Sherafat MH, Guitel R, Quaegebeur N, Hubert P, Lessard L, Masson P. Structural health monitoring of a composite skin-stringer assembly using within-the-bond strategy of guided wave propagation. Mater Des 2016;90:787–94.
[9] Roth W, Giurgiutiu V. Structural health monitoring of an adhesive disbond through electromechanical impedance spectroscopy. Int J Adhes Adhes 2017;73(November 2016):109–17.
[10] Carrino S, Nicassio F, Scarselli G, Vitolo R. Finite difference model of wave motion for structural health monitoring of single lap joints. Int J Solids Struct 2019;161:219–27.
[11] Sam-Daliri O, Farahani M, Faller LM, Zangl H. Structural health monitoring of defective single lap adhesive joints using graphene nanoplatelets. J Manuf Process 2020;55(December 2019):119–30.
[12] De Simone ME, Andreades C, Meo M, Ciampa F. Smart composite detector of orbital debris and micrometeoroids particles. Mater Today Proc 2020:2–9.
[13] Di Sante R. Fibre optic sensors for structural health monitoring of aircraft composite structures: recent advances and applications. Sensors 2015;15(8):18666–713.
[14] Su LYZ. Identification of Damage Using Lamb Waves, vol. 49. Berlin: Springer; 2009.
[15] Guo JYH, Xiao G, Mrad N. Fiber optic sensors for structural health monitoring of air platforms. Sensors 2011;11:3687–705.
[16] Hafizi ZM, Epaarachchi J, Lau KT. Impact location determination on thin laminated composite plates using an NIR-FBG sensor system. Meas J Int Meas Confed 2015;61:51–7.
[17] Ren Z, Li J, Zhu R, Cui K, He Q, Wang H. Phase-shifting optical fiber sensing with rectangular-pulse binary phase modulation. Opt Lasers Eng 2018;100:170–5.
[18] Maheshwari M, Annamdas VGM, Pang JHL, Asundi A, Tjin SC. Crack monitoring using multiple smart materials; fiber-optic sensors & piezo sensors. Int J Smart Nano Mater 2017;8:41–55.
[19] Jang BW, Kim CG. Real-time detection of low-velocity impact-induced delamination onset in composite laminates for efficient management of structural health. Compos Part B Eng 2017;123:124–35.
[20] Nag-Chowdhury S, Bellegou H, Pillin I, Castro M, Longrais P, Feller JF. Non-intrusive health monitoring of infused composites with embedded carbon quantum piezo-resistive sensors. Compos Sci Technol 2016;123:286–94.
[21] Zhou G, Sim LM. Damage detection and assessment in fibre-reinforced composite structures with embedded fibre optic sensors — review. Smart Mater Struct 2002;11:925–39.
[22] Chambers AR, Mowlem MC, Dokos L. Evaluating impact damage in CFRP using fibre optic sensors. Compos Sci Technol 2007;67(6):1235–42.
[23] Hirsch M, Majchrowicz D, Wierzba P, Weber M, Bechelany M, Jędrzejewska-Szczerska M. Low-coherence interferometric fiber-optic sensors with potential applications as biosensors. Sensors (Switzerland) 2017;17(2):1–12.
[24] Giurgiutiu V. Fiber-optic sensors. In: Structural Health Monitoring of Aerospace Composites; 2016, p. 249–96.
[25] Kocaman ES, et al. Monitoring the damage state of fiber reinforced composites using an FBG network for failure prediction. Materials (Basel) 2017;10(32):1–19.
[26] Güemes A, Fernández-López A, Díaz-Maroto PF, Lozano A, Sierra-Perez J. Structural health monitoring in composite structures by fiber-optic sensors. Sensors (Switzerland) 2018;18(4):1–11.
[27] Shivakumar K, Bhargava A. Failure mechanics of a composite laminate embedded with a fiber optic sensor. J Compos Mater 2005;39(9):777–98.
[28] Liu R-m, Liang D-k. Natural frequency detection of smart composite structure by small diameter fiber Bragg grating. J Vib Control 2014;January.
[29] Takeda S, Okabe Y, Takeda N. Delamination detection in CFRP laminates with embedded small-diameter fiber Bragg grating sensors. Compos Part A 2002;33(December 2013):971–80.
[30] T60/ Small Diameter Fiber (Thin) FBG, Technica. [Online]. Available: https://technicasa.com/t60-small-diameter-fiber-thin-fbg/. [Accessed: 11-Dec-2020].
[31] Ramly R, Kuntjoro W, Rahman MKA. Using embedded fiber bragg grating (FBG) sensors in smart aircraft structure materials. Procedia Eng 2012;41(Iris):600–6.
[32] Miguel Giraldo C, Zúñiga Sagredo J, Sánchez Gómez J, Corredera P. Demonstration and methodology of structural monitoring of stringer runs out composite areas by embedded optical fiber sensors and connectors integrated during production in a composite plant. Sensors 2017;17(1683):1–22.
[33] Goossens S, et al. Aerospace-grade surface mounted optical fibre strain sensor for structural health monitoring on composite structures evaluated against in-flight conditions. Smart Mater Struct 2019;28(6).
[34] Qiu Y, Wang Q, Zhao H, Chen J, Wang Y. Review on composite structural health monitoring based on fiber Bragg grating sensing principle. J Shanghai Jiaotong Univ 2013;18(2):129–39.
[35] Boateng EKG, Schubel P, Umer R. Thermal isolation of FBG optical fibre sensors for composite cure monitoring. Sensors Actuators, A Phys 2019;287:158–67.
[36] Alberto NJ, Marques CA, Pinto JL, Nogueira RN. Three-parameter optical fiber sensor based on a tilted fiber Bragg grating. Appl Opt 2010;49(31):6085–91.
[37] Min R, Ortega B, Marques C. Fabrication of tunable chirped mPOF Bragg gratings using a uniform phase mask. Opt Express 2018;26(4):4411–20.
[38] Markowski K, Jędrzejewski K, Marzęcki M, Osuch T. Linearly chirped tapered fiber-Bragg-grating-based Fabry-Perot cavity and its application in simultaneous strain and temperature measurement. Opt Lett 2017;42(7):1464–7.
[39] Tan RX, et al. Birefringent Bragg grating in C-shaped optical fiber as a temperature-insensitive refractometer. Sensors 2018;18(3285).
[40] Tressler JF, Qin L, Uchino K. Piezoelectric composite sensors, no. May 2015. Elsevier Ltd.; 2016.
[41] Ramadan KS, Sameoto D, Evoy S. A review of piezoelectric polymers as functional materials for electromechanical transducers. Smart Mater Struct 2014;23(3).
[42] Masmoudi S, El Mahi A, Turki S. Fatigue behaviour and structural health monitoring by acoustic emission of E-glass/epoxy laminates with piezoelectric implant. Appl Acoust 2016;108:50–8.
[43] Qiu L, Deng X, Yuan S, Huang Y, Ren Y. Impact monitoring for aircraft smart composite skins based on a lightweight sensor network and characteristic digital sequences. Sensors 2018;18(2218):1–27.
[44] Giurgiutiu V. Piezoelectric wafer active sensors. In: Structural Health Monitoring of Aerospace Composites. USA: Elsevier; 2016. p. 177–248.
[45] Annamdas VGM, Soh CK. Application of electromechanical impedance technique for engineering structures: review and future issues. J Intell Mater Syst Struct 2010;21(1):41–59.
[46] Wandowski T, Malinowski PH, Ostachowicz WM. Temperature and damage influence on electromechanical impedance method used for carbon fibre-reinforced polymer panels. J Intell Mater Syst Struct 2017;28(6):782–98.
[47] de Oliveira MA, Monteiro AV, Filho JV. A new structural health monitoring strategy based on PZT sensors and convolutional neural network. Sensors (Switzerland) 2018;18(9).
[48] Wandowski T, Malinowski PH, Ostachowicz WM. Delamination detection in CFRP panels using EMI method with temperature compensation. Compos Struct 2016;151:99–107.
[49] Iurgiutiu VIG. Electro-mechanical impedance method for crack detection in thin plates. J Intell Mater Syst Struct 2015;12:709–18.
[50] Thomas GR, Khatibi AA. Durability of structural health monitoring systems under impact loading. Procedia Eng 2017;188:340–7.
[51] Carboni M, Gianneo A, Giglio M. A Lamb waves based statistical approach to structural health monitoring of carbon fibre reinforced polymer composites. Ultrasonics 2015;60:51–64.
[52] Smart Material, Smart Material - Home of the MFC, MFC - Macro Fiber Composite. [Online]. Available: https://www.smart-material.com/MFC-product-main.html. [Accessed: 18-Dec-2019].
[53] Lin M, Qing X, Kumar A, Beard SJ. SMART layer and SMART suitcase for structural health monitoring applications. In: Smart Structures and Materials 2001: Industrial and Commercial Applications of Smart Structures Technologies, vol. 4332; 2001, p. 98–106.
[54] Qing XP, Beard SJ, Kumar A, Chan HL, Ikegami R. Advances in the development of built-in diagnostic system for filament wound composite structures. Compos Sci Technol 2006;66(11–12):1694–702.
[55] Wang Y, Qiu L, Luo Y, Ding R. A stretchable and large-scale guided wave sensor network for aircraft smart skin of structural health monitoring. Struct Heal Monit 2019:1–16.
[56] Jung KC, Chang SH. Performance evaluation of smart grid fabrics comprising carbon dry fabrics and PVDF ribbon sensors for structural health monitoring. Compos Part B Eng 2019;163:690–701.
[57] Lambinet F, Khodaei ZS. Smart patch repair with low profile PVDF sensors. Key Eng Mater 2017;754:359–62.
[58] Avilés F, May-pat A, López-manchado MA, Verdejo R, Bachmatiuk A. A comparative study on the mechanical, electrical and piezoresistive properties of polymer composites using carbon nanostructures of different topology. Eur Polym J 2018;99(September 2017):394–402.
[59] Teixeira J, Horta-romarís L, Abad M, Costa P, Lanceros-méndez S. Piezoresistive response of extruded polyaniline/ (styrene-butadiene-styrene) polymer blends for force and deformation sensors. Mater Des 2018;141:1–8.
[60] Nonn S, Schagerl M, Zhao Y, Gschossmann S, Kralovec C. Application of electrical impedance tomography to an anisotropic carbon fiber-reinforced polymer composite laminate for damage localization. Compos Sci Technol 2018;160:231–6.
[61] Peng TCH, Li Q. Carbon nanotubes for defect monitoring in fiber-reinforced polymer composites. In: Industrial Applications of Carbon Nanotubes, vol. 437, no. June. Amsterdam: Elsevier; 2017, pp. 71–100.
[62] Balaji R, Sasikumar M. Graphene based strain and damage prediction system for polymer composites. Compos Part A 2017;103:48–59.
[63] Moriche R, Sánchez M, Jiménez-Suárez A, Prolongo SG, Ureña A. Electrically conductive functionalized-GNP/epoxy based composites: from nanocomposite to multiscale glass fibre composite material. Compos Part B Eng 2016;98:49–55.
[64] Jan R, et al. Liquid exfoliated graphene smart layer for structural health monitoring of composites. J Intell Mater Syst Struct 2017;28(12):1565–74.
[65] Montazerian H, Rashidi A, Dalili A, Najjaran H, Milani AS, Hoorfar M. Graphene-coated spandex sensors embedded into silicone sheath for composites health monitoring and wearable applications. Small 2019;15(1804991):1–12.

[66] Luo S, Liu T. Graphite nanoplatelet enabled embeddable fiber sensor for in situ curing monitoring and structural health monitoring of polymeric composites. ACS Appl Mater Interfaces 2014;6(12):9314–20.
[67] Cagáň J, Pelant J, Kyncl M, Kadlec M, Michalcová L. Damage detection in carbon fiber–reinforced polymer composite via electrical resistance tomography with Gaussian anisotropic regularization. Struct Heal Monit 2019;18(5–6):1698–710.
[68] Baltopoulos A, Polydorides N, Pambaguian L, Vavouliotis A, Kostopoulos V. Damage identification in carbon fiber reinforced polymer plates using electrical resistance tomography mapping. J Compos Mater 2013;47(26):3285–301.
[69] Cagáň J. Hardware implementation of electrical resistance tomography for damage detection of carbon fibre–reinforced polymer composites. Struct Heal Monit 2017;16(2):129–41.
[70] Loyola BR, La Saponara V, Loh KJ, Briggs TM, Bryan GO, Skinner JL. Spatial sensing using electrical impedance tomography. IEEE Sens J 2013;13(6):2357–67.
[71] Thostenson E, Chou T. Carbon nanotube networks: sensing of distributed strain and damage for life prediction and self healing. Adv Mater 2006;18:2837–41.
[72] Chou TW, Gao L, Thostenson ET, Zhang Z, Byun JH. An assessment of the science and technology of carbon nanotube-based fibers and composites. Compos Sci Technol 2010;70(1):1–19.
[73] Zhang H, Liu Y, Kuwata M, Bilotti E, Peijs T. Improved fracture toughness and integrated damage sensing capability by spray coated CNTs on carbon fibre prepreg. Compos Part A 2015;70:102–10.
[74] Baltopoulos A, Polydorides N, Pambaguian L, Vavouliotis A, Kostopoulos V. Exploiting carbon nanotube networks for damage assessment of fiber reinforced composites. Compos Part B Eng 2015;76:149–58.
[75] Naghashpour A, Van Hoa S. A technique for in-situ detection of random failure in composite structures under cyclic loading. J Compos Mater 2019;53(23):3243–55.
[76] Takeda T, Narita F. Fracture behavior and crack sensing capability of bonded carbon fiber composite joints with carbon nanotube-based polymer adhesive layer under Mode I loading. Compos Sci Technol 2017;146:26–33.
[77] Alexopoulos ND, Bartholome C, Poulin P, Marioli-Riga Z. Structural health monitoring of glass fiber reinforced composites using embedded carbon nanotube (CNT) fibers. Compos Sci Technol 2010;70(2):260–71.
[78] Sebastian J, et al. Health monitoring of structural composites with embedded carbon nanotube coated glass fiber sensors. Carbon N Y 2014;66:191–200.
[79] Luo S, Obitayo W, Liu T. SWCNT-thin-film-enabled fiber sensors for lifelong structural health monitoring of polymeric composites - From manufacturing to utilization to failure. Carbon 2014;76:321–9.
[80] Moriche R, Jiménez-Suárez A, Sánchez M, Prolongo SG, Ureña A. Graphene nanoplatelets coated glass fibre fabrics as strain sensors. Compos Sci Technol 2017;146:59–64.
[81] NETZSCH, DEA 288 Ionic - Dielectric Analyzer - NETZSCH Analyzing & Testing. [Online]. Available: https://www.netzsch-thermal-analysis.com/en/products-solutions/dielectric-analysis/dea-288-ionic/. [Accessed: 22-Jun-2020].
[82] Ali MA, Umer R, Khan KA, Samad YA, Liao K, Cantwell W. Graphene coated piezo-resistive fabrics for liquid composite molding process monitoring. Compos Sci Technol 2017;148:106–14.
[83] Yang Y, et al. Design and integration of flexible sensor matrix for in situ monitoring of polymer composites. ACS Sensors 2018;3(9):1698–705.
[84] Carlone P, Palazzo GS. Unsaturated and saturated flow front tracking in liquid composite molding processes using dielectric sensors. Appl Compos Mater 2015;22(5):543–57.
[85] Carlone P, Rubino F, Paradiso V, Tucci F. Multi-scale modeling and online monitoring of resin flow through dual-scale textiles in liquid composite molding processes. Int J Adv Manuf Technol 2018;96:2215–30.
[86] Qing X, Liu X, Zhu J, Wang Y. In-situ monitoring of liquid composite molding process using piezoelectric sensor network. Struct Heal Monit 2020;(411).
[87] Wang JC, Molimard P, Drapier J, Vautrin S, Minni A. Monitoring the resin infusion manufacturing process under industrial environment using distributed sensors. J Compos Mater 2012;46(6):691–706.
[88] Tifkitsis KI, Skordos AA. A novel dielectric sensor for process monitoring of carbon fibre composites manufacture. Compos Part A Appl Sci Manuf 2019;123:180–9.
[89] Fu H, Sharif Khodaei Z, Aliabadi MHF. An event-triggered energy-efficient wireless structural health monitoring system for impact detection in composite airframes. IEEE Internet Things J 2019;6(1):1183–92.
[90] Rusci M, Rossi D, Farella E, Benini L. A sub-mW IoT-endnode for always-on visual monitoring and smart triggering. IEEE Internet Things J 2017;4(5):1284–95.
[91] Pughat A, Sharma V. Performance analysis of an improved dynamic power management model in wireless sensor node. Digit Commun Networks 2017;3:19–29.
[92] Dragos K, Theiler M, Magalhães F, Moutinho C, Smarsly K. On-board data synchronization in wireless structural health monitoring systems based on phase locking. Struct Control Heal Monit 2018;25(11):1–19.
[93] Le MQ, et al. Review on energy harvesting for structural health monitoring in aeronautical applications. Prog Aerosp Sci 2015;79:147–57.